Nanofiber Inclusion and Fiber Pore Volume Potential to Affect Fundamental Filtration of NaCl Aerosols

by

Amulya Poudyal

A thesis submitted to the Graduate Faculty of
Auburn University
in partial fulfillment of the
requirements for the Degree of
Master of Science

Auburn, Alabama
December 14, 2019

Keywords: sea salt aerosol filtration, nano-fiber inclusion, pore volume of ACF, quality factor, particles loading capacity, filter regeneration

Approved by

Bruce J. Tatarchuk, Chair, Professor of Chemical Engineering
Maria Auad, Professor of Chemical Engineering
Zhihua Jiang, Assistant Professor of Chemical Engineering

Abstract

Sea salt aerosols are generated when the high-speed vessels travelling in the ocean collide with white caps from wake or bow of the ships. These aerosols have salt particulates ranging from 0.1 to 10 microns. These high-speed vessels have many air breathing equipment such as SOFS, turbines etc. If unfiltered, these salt particulates will flow into these equipment and deposit on the turbines or cathodes of fuel cells, deleteriously affecting its performance and decreasing its lifetime. Therefore, it is critical to remove these particulates before it is consumed by the air breathing equipment.

Commercial filter media have been used to address this problem. However, the commercial filter media are surface filters without any depth. These filters can hold limited amount of salt particles, before reaching unacceptable levels of pressure drop. Newly designed vessels are anticipated to ingest even higher level of impurities, further increasing the rate of performance degradation. Hence the development of new and improved filtration materials and methodologies are vital.

As a solution to this problem, an attempt was made in our lab to synthesize and evaluate a novel three-dimensional, asymmetric, porous, microfibrous filter media consisting of nanofibers embedded within microfibrous network. Nano-fiber flocs made of Vapor Grown Carbon Fibers (VGCFs) fibers were embedded with activated carbon fibers and polyester fibers to synthesize these novel filter media. Activated carbon fibers are porous in nature and hydrophilic. They can wick the salt aerosol into its pore via capillary forces. Hence this porous nature of the activated carbon helps to trap even more particulates, compared to a non-porous fiber. As long as the nano-fibers are wet, the salt loading process continues until the saturation occurs in the pores. This is a novel phenomenon, because a significant amount of salt particulates can be trapped inside the

pores without any pressure drop penalty. Hence in AU nano-floc filter media, the pores of activated carbon and the interstitial spaces between fibers are utilized first, before surface filtration takes place. This results in the particle loading capacity of AU nano-floc media to be significantly higher than that of the commercial GOTs media. The loading of particles into the pores and the interstitial spaces between the fibers is referred as volume filtration mechanism. The volume filtration mechanism contributes in holding significant amount of salt particulates without reaching unacceptable levels of pressure drops.

This work discusses the efforts and summarizes the results associated with the inclusion of nanofiber for enhanced salt removal, the potential of porous nature of activated carbon fibers in salt entrapment and the regeneration ability of nanofiber filters. Fundamental filtration performance metrics such as filtration removal efficiency, Quality Factor (QF) etc. have been used to quantify the results. Additionally, another critical filtration parameter i.e. particle loading capacity has also been included in the studies. Experiments were performed to study the filtration performance of nano-floc filters on both wet and dry sea salt aerosols over a range of relative humidity and face velocity encountered by high-speed vessels. In addition, inclusion of hydrophobic material Polytetrafluoroethylene (PTFE) was also investigated to examine its ability to prevent aqueous flooding, enhance filtration and resist clogging. Most importantly, these novel wet-laid nanofiber filters were tested under relevant Navy test conditions and performance metrics were obtained and compared against the commercial GOTS media.

Acknowledgments

I would like to express sincere gratitude to Dr Bruce J. Tatarchuk for his guidance throughout the course of this research. I would like to acknowledge Office of Naval Research for funding the research presented in this thesis. I would also like to thank Dr Maria Auad and Dr Zhihua Jiang for serving on my thesis committee.

I would like to thank Dr. Wenhua Zhu for his invaluable support in every step of my research. I would also like to thank Dr Mario Eden and Mrs. Elaine Manning for academic support. I would like to thank my mother Kabita Dhakal Poudyal and father Tanka Nath Poudyal for their constant love and support, without which this would not have been possible. Lastly, I would like to thank my best friend Shivani Aryal for believing in me, for encouraging me and always being there for me.

Table of Contents

List of Tables

List of Figures

List of Abbreviations

ACF	Activated Carbon Fibers
VGCF	Vapor Grown Carbon Fibers
QF	Quality Factor
MPPS	Most Penetrating Particle Size
PTFE	Polytetrafluoroethylene
LCAC	Landing Craft Air Cushion
RH	Relative Humidity
AU	Auburn University
SDS	Sodium Dodecyl Sulfate
CTAB	Cetrimonium Bromide
SEM	Scanning Electron Microscope
HEPA	High Efficiency Particulate Air
UPLA	Ultra Low Particulate Air
CCVD	Catalytic Chemical Vapor Deposition
SMM	Sintered Metal Microfibrous

Chapter 1: Introduction to Sea Salt Aerosol Filtration

1.1 Background

Particle free air is important aboard high-speed vessels operating in a humid environment which is abundant in salt aerosols. The high-speed vessels contain many air breathing equipment like fuel cells, turbines etc. For applications that demand high removal of contaminants, common practice is to use filters with activated carbon and/or other chemically active materials.[35] Sea salt aerosols are in the particle size range of 0.1 to 10 microns.[2]

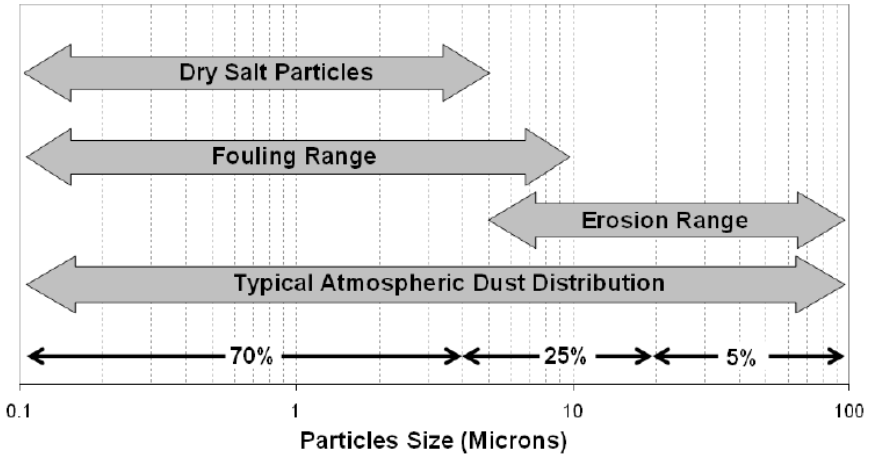

Figure 1. Typical particle size distribution for erosion and fouling range[2]

With advancement in technologies, newer vessels operating at higher speed are expected to ingest even higher levels of salt particulates. Hence, novel filter media with fundamentally new filtration mechanism is vital. Therefore, the primary focus of this thesis is to investigate the effect of nanofiber inclusion on filtration media for sea salt aerosol filtration and the potential of the pore volume of activated carbon fibers to entrap salt aerosol. All of the topics discussed in this thesis fall under one of these two novel filtration mechanisms.

1.1.1 Importance of Sea Salt Aerosol Filtration

Sea salt aerosols and particulates have been a substantial problem for different Naval operations. High-speed Navy vessels like LCAC, combat ships operate in ocean environment

where there are excessive amounts of salt in the air, in the form of aerosol. These aerosols are generated from the wind stresses over whitecaps or from wake or bow spray by ship itself.[1] Sea salt deleteriously affects turbine engines as well as a host of air breathing equipment for power supply, instrumentation, propulsion and personnel. The salt particulates can deposit onto the turbines and cathode of the fuel cells and cause corrosion, hence degrading performance, decreasing lifetime and increasing maintenance and operation costs.

Figure 2. Ship in the ocean with large wake and bow spray[1]

Larger particulates and aerosols (ca. > 2μm) can be readily removed using large particle continuous filter systems like cyclones, inertial coalesers, moisture separators, chevron filters, louvers and meshes etc. These large particle continuous filtration systems are mostly inertial systems which can handle significant amounts of contaminants without any issue of clogging or end of life and can be continuously refreshed. However, particulates below 2 μm are difficult to filter. Conventionally small barrier filters have been employed in conjunction with large particulate filters, however these small particulate filters have a low dirt holding capacity and reach unacceptable levels of pressure drops quickly, as a result of filter cake formation.

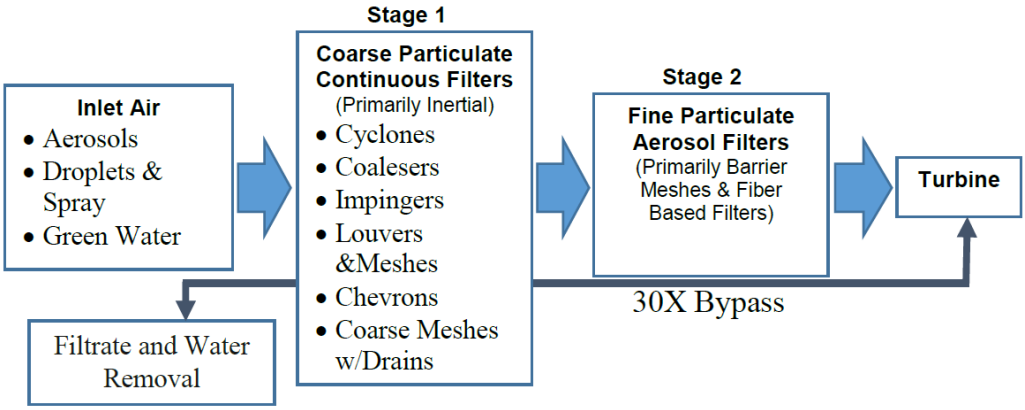

Figure 3. Two Stage Filtration System Utilizing Continuous Inertial Filters Followed by a Fine Particle Barrier Filter Bank

The formation of filter cake stresses the flow of salt aerosol through the lower pressure drop leakage pathways and into the turbines. These leaked salt particulates ingested by turbines have been found to be as much as 30 times higher than expected. With new classes of high-speed vessels, the amount of salt aerosol ingested will increase further, worsening the situation. Hence there is a vital need for improved filters with higher salt holding capabilities. These enhanced filters can decrease M&O cost, decrease replacement costs and increase the lifetime of the equipment.

1.1.2 History of Aerosol Filtration

History of aerosol filtration is over 2000 years old, almost dating back to Roman times. “Industrial dust” in mines in Egypt was mentioned in Natural History of Pliny the Elder (ca a.d. 50) and Julius Pollux (ca a.d. 150) who proposed loose bladders for preventing dust inhalation. Leonardo da Vinci introduced wet clothes as protection from fumes used in warfare. In 1860 Louis Pasteur demonstrated the need of medical respirators to prevent airborne organism from causing putrefaction. Smoke filters were developed in the 19th century to protect firefighters from fire smoke. Gas masks and respirators were used to prevent inhalation of toxic chemicals during World

War I. Fibrous pads was developed in 1930 in Germany which used adsorption as filtration mechanism. Hansen in 1930 discovered that powdering wood filter pad with resin increased filtration efficiency. During World War II several types of fibrous materials in different forms were used as fibrous filters. Pore filters like cellulose membrane, metal membrane etc. were also developed for separating fine particles dispersed in gases.[4,6]

Filtration mechanisms also have a long history. Brownian motion was studied in early 1800s. In 1920s it was discovered that maximum penetration occurred at 0.1-0.2 μm particle radius. Kaufman, in 1936, combined theories of small particle filtration by Brownian motion and larger particles by inertial impingement. Particle diffusion and direct interception was proposed by Langmuir in 1942, 1946. Isolated fiber theories were developed by Davies in 1950s. Yoshika studied the effects of gravitational deposition and clogging in 1970s. Darcy law was used to initially describe filter resistance. Pich in 1966 related pressure drop to Knudsen number. Description of airflow field through fiber filter was made by Kuwabara in 1959. Since then many different theories regarding new concepts of filtration, resistance, adhesion of particles, testing methods etc. have been developed and is still being developed.[4,6]

1.1.3 Different Types of Aerosol Filters

There are five different types of aerosol filters based on their structures. Screen filters use polymer or metal screen for filtration and are used for low-efficiency and cake filtration. Granular filters are packed bed filters with large particles used for high temperature chemical processes. Due to low voidage, granular filters have high pressure drops. Sintered metal filters are made by sintering metal spheres together, but they are expensive. Membrane/pore filters are made from porous plastics and foams for high filtration efficiency requiring applications but are costly. Fibrous filters are made of woven or non-woven fabrics. These filters have high voidage resulting

in high air permeability, which implies less loss of energy in the form of pressure drop across filter. These filters are low cost and easy to manufacture on large scale. In particular, non-woven media are gaining more popularity since they can be made using variety of materials such as cellulose, polymer, glass and/or metal fibers. This flexibility of material along with ease of manufacturing has made non-woven a preferred choice. Removal efficiency of >95% is desired for sea salt aerosol, since even small amounts of salt particulates can cause serious problems for equipment in long term. Hence nano-fiber nonwoven filter media was investigated as a part of this thesis.

1.1.4 Fundamentals Mechanisms of Filtration

Sea salt particulates range in diameter from 0.1 to 10 μm. The filtration of particulates below 2 μm, and specifically in the ca. 0.1 to 0.3 μm (MPPS), is a fundamentally much more difficult and challenging task. Figure 4 demonstrates four predominant fundamental filtration mechanisms.

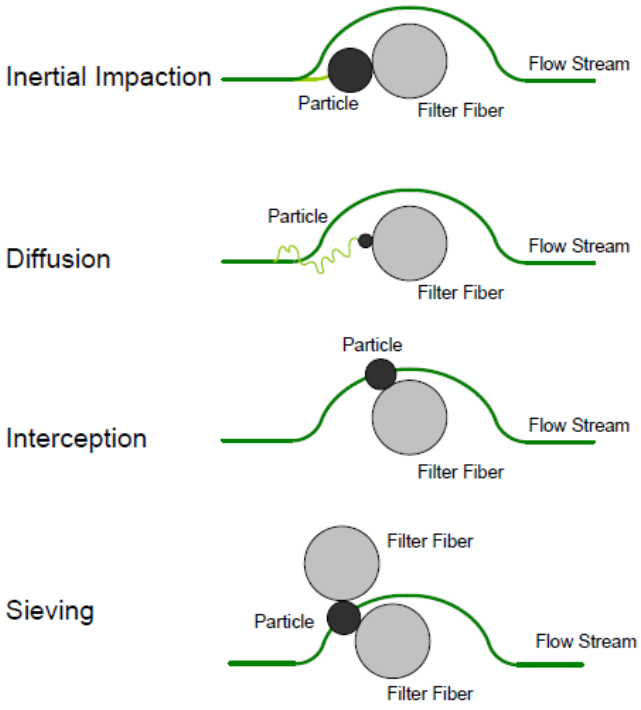

Figure 4. Common filtration mechanisms[2]

The sieving mechanism requires extremely low contaminants loads to be effective long term. For particulates below 2 μm, three fundamental filtration mechanisms: Inertial Impaction, Interception and Diffusion, come into play simultaneously. Inertial impaction applies to particles larger than 1 μm. This mechanism occurs for particle with high inertia/momentum which causes it to divert it from the streamline and collide with the fiber. The particulates flow in a straight path, and once it reaches close to the fiber, they leave the flow path due to inertia and impacts the filter fiber where it is attached and held in place, as shown in Figure 4.[2] Diffusion mechanism is primary mechanism for particulates less than 0.1 μm diameter. These particulates are not held by viscous forces in the fluid and can diffuse randomly within the flow stream, depending on its interaction with nearby particulates and gas molecules. These diffusing particulates collide with the fibers and are captured.[2] The diffusion refers to Brownian motion of small particles to the fibers where they are attracted and held by van der Waal's force. Brownian motion occurs when the aerosol particle size is comparable to the mean free path of gas molecules (0.06 μm in air).[4] The random path during Brownian motion is longer than the streamline path, hence the probability of the particles to get captured is very high. Particle greater than 0.3 μm in diameter do not have significant Brownian motion in air. Interception mechanism refers to the phenomenon when particle flowing in the fluid streamline gets captured by the filter fiber when it comes within one particle radius of the filter fiber. It is one of the main mechanisms for mid-sized particulates (between 0.1 and 1 μm in diameter) which are not bigger enough for inertial impaction but are not smaller enough to diffuse. These particulates will just follow the flow stream, touch the fiber and get trapped.[2] This mechanism is applicable only for streamlines that are close enough to the filter fiber.

There also exists a fifth kind of mechanism called electrostatic deposition, which is based on the charge of the filter fiber and the particles. A charged fiber can attract a counter charged

particle by inducing electric field. It can also attract counter charged particle via image effect of charge.[4] Electrostatic filters have the advantage of increasing the filtration efficiency without increasing pressure drop. However, these filters are less reliable due to decreased filtration efficiency as a result of loss of charge with time. The loss of charge can be caused due to neutralization and/or dirt coverage on fibers. Also scaling up of these filters on manufacturing scale is difficult.[35] Gravitational settling is another mechanism which is only effective for particulates above 10 μm in diameter.

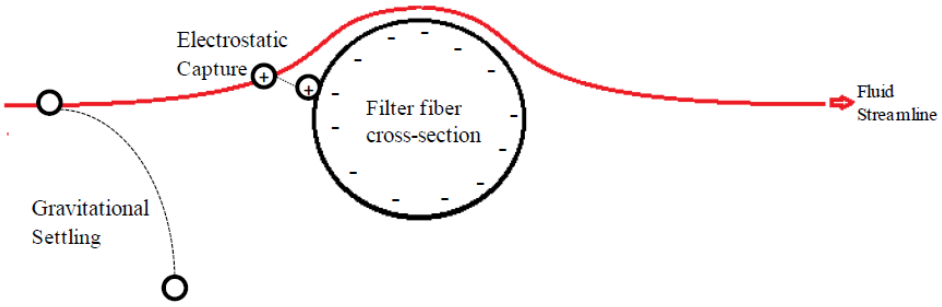

Figure 5. Electrostatic capture and gravitational settling mechanisms[35]

Since we are dealing with salt aerosols, the three most important filtration mechanisms that take place are diffusion, interception and inertial impaction. The dominant filtration mechanism depends on the aerosol particle size. There exists a range in the 0.04 to 0.4 μm particle diameter where no mechanism is strong enough to remove the particle. This phenomenon occurs because particles in this range are too small to be removed by inertial effects and are too large to for Brownian motion to assist them in leaving the flow stream to encounter the filter fibers. There is a dip in the filtration efficiency curve denoting this range. The particle size corresponding to the lowest point on the dip is called the Most Penetrating Particle Size (MPPS) which has the lowest filtration efficiency value.

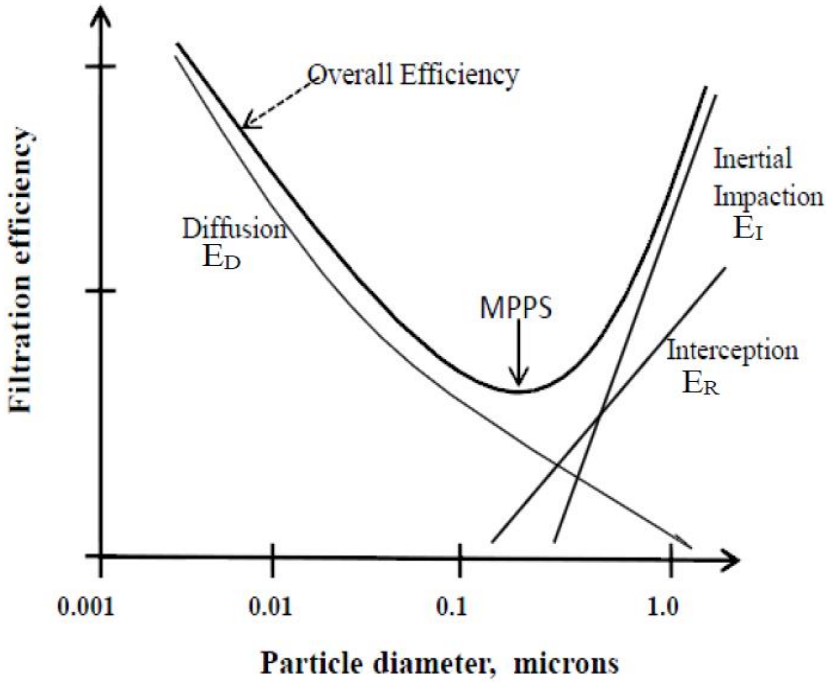

Figure 6. Most Penetrating Particle Size (MPPS) region on the combined filtration efficiency curve resulting from diffusion, inertial impaction and interception mechanisms[35]

The MPPS is a result of interplay of the fundamental physical behavior of particles flowing through the fiber-based filter which is the focus of this thesis. Specifically, the work focuses on the incorporation of nanomaterials into the filter media, elucidates the porous nature of activated carbon fibers, investigates the regenerative capability of nano-floc embedded filters and demonstrates the particle loading capacity of nano-floc filters.

1.1.5 Filtration Performance Metrics

The parameters optimized during fibrous filter designs are filtration efficiency, pressure drop/resistance, Quality Factor and particle loading capacity. These parameters can be optimized based on the requirements of air quality.

1.1.5.1 Filtration Efficiency

The filtration efficiency is the most important metric used to measure the performance of a filter. It primarily depends on type of filter media used. It also depends on particle size of

filtrate, filtration area and filtration velocity. The average filtration efficiency can be evaluated using equation 1, according to ASHRAE 52.2 Standard[17]. It is expressed as a number between 0 and 1. Theoretically filtration efficiency has been modeled by Total Filtration Efficiency Model and is discussed in the following section.

$$E = \left(\frac{n_{up} - n_{down}}{n_{up}}\right) \qquad Equation\ 1$$

1.1.5.1.1 Total Filtration Efficiency Model (Theoretical Model)

The total filtration efficiency model, given by equation 2, describes the combined influences of inertial impaction, diffusion and interception mechanisms for removing particulates below 2 μm.[2-6]

Total Filtration Efficiency[15,16] $E = 1 - exp\left(\frac{-4\alpha E_{\Sigma} t}{\pi R}\right)$ $Equation\ 2$

where α is the fiber packing density (dimensionless), t is the filter thickness in m, R is the fiber diameter in m, E_{Σ} is total single fiber efficiency and includes the contributions of all the mechanisms noted above. E_{Σ} is dimensionless and is a number between 0 and 1, with 1 being 100% removal efficiency.

Single Fiber Efficiency [15,16] $E_{\Sigma} = 1 - (E_D)(E_R)(E_I)$

where E_D stands for efficiency of diffusion, E_R stands for efficiency of interception and E_I stands for efficiency of inertial impaction

Efficiency of diffusion mechanism $E_D = 1.6\left(\frac{1-\alpha}{Ku}\right)^{\frac{1}{3}} Pe^{-\frac{2}{3}} C_d C_d{}''$

where $C_d = 1 + 0.388 Kn_f\left(\frac{(1-\alpha)Pe}{Ku}\right)$ and $C_d{}'' = \frac{1}{1+A\left(\frac{1-\alpha}{Ku}\right)^{\frac{1}{3}} Pe^{-\frac{2}{3}} C_d}$

Efficiency of interception mechanism $E_R = 0.6\,\frac{1-\alpha}{Ku}\,\frac{R^2}{1+R}$ $R = \frac{d_p}{d_f}$

Efficiency of inertial impaction mechanism $E_I = 0.0334 Stk^{\frac{3}{2}}$

The dimensionless numbers in the above equations are defined as follows:

Peclet number: $Pe = \frac{Ud_f}{D}$

Stokes number: $Stk = \frac{\rho_p {d_p}^2 U}{18\mu d_f}$

Kuwabara number: $Ku = -ln\left(\frac{\alpha}{2}\right) - 0.75 + \alpha - 0.25\alpha^2$

Knudsen number: $Kn_f = 2\frac{\lambda}{d_f}$

where U is the air flow velocity in m/s, D is the coefficient of Brownian diffusion in m^2/s, λ is the gas mean free path, α is the packing density (unitless), ρ_p is the particle density in kg/m^3, μ is the air flow viscosity in Pa.s, d_p is the diameter of the aerosol particle and d_f is the fiber diameter in m respectively.

1.1.5.2 Pressure Drop

The filtration efficiency is directly proportional to pressure drop across the filter media. Pressure drop across a filter media corresponds directly to the energy consumption since it is indicative of the work done by the blower to push air through the filter[11]. There is a tradeoff between pressure drop and filtration efficiency, hence an optimization must be done for optimal filtration performance. Pressure drop across a filter media is a function of face velocity of air passing through it and is related by Equation 3, known as Darcy's law[12].

$$\Delta P = AV_M \qquad Equation\ 3$$

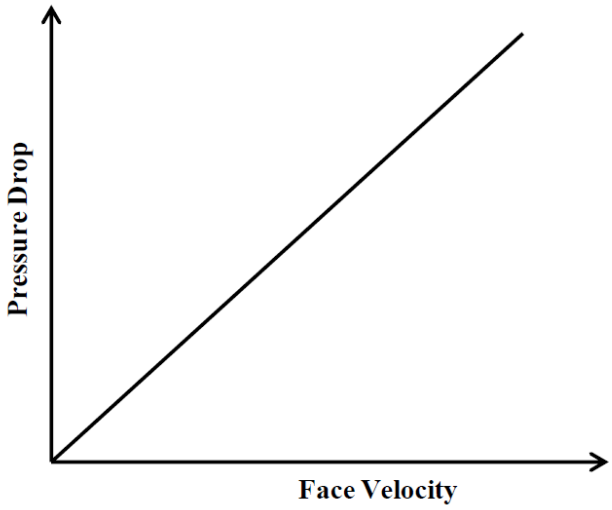

Figure 7. Pressure drop profile across filter according to Darcy's law

Figure 7 shows that according to Darcy's law, the pressure drop across the filter varies linearly with face velocity. Quadratic and third order dependence of pressure drop with high velocities may be seen due to compression of the filter media or due to filter design.

1.1.5.3 Quality Factor

Filtration process consumes energy in the form of pressure drop (i.e. PV work). The cost-benefit ratio of filtration process is defined in terms of Quality Factor, which is defined by equation 4. The Quality Factor is fundamentally defined as filtration efficiency divided by the pressure drop through the media. Quality Factor can also be defined as the ratio of fractional capture of particles per unit thickness divided by the pressure drop per unit thickness.

$$QF = \frac{\gamma}{\Delta P/_t} = \frac{\gamma t}{\Delta P} = \frac{\ln(1/P)}{\Delta P} = -\frac{\ln\left(\frac{1}{E}\right)}{\Delta P} \qquad Equation\ 4$$

where γ is the fractional capture of particle per thickness (dimensionless), t is filter thickness in m, ΔP is pressure drop across the filter in Pa, E is the total filtration efficiency (dimensionless).

The Quality Factor can depend on many variables including: gas temperature, gas pressure, gas face velocity, gas viscosity, RH, particulate size, particulate composition, particulate shape and many filter properties including fiber diameter, composition, orientation, volume loading, media thickness, hydrodynamic entrance, exit conditions etc. The Quality Factor also incorporates the fundamental filtration mechanisms discussed above.

1.1.5.4 Particle Loading Capacity

The filtration efficiency, pressure drop, and Quality Factor changes with time, as more particulates get entrapped by the filters[3]. Particle loading capacity is defined as the quantity of contaminant a filter can trap and hold before the maximum allowable back pressure drop is reached. It is indicative of the filter lifetime[13]. As the particle loaded into the filter increases, the pressure drop across the filter media also increases. Hence, depending on the power consumption, the upper limit to pressure drop is defined, after which the filter is replaced. Filters with high particle loading capacity is desired, but these filters also have low filtration efficiency. Hence an optimization should be performed according to both parameters. Different fiber materials and packing densities can lead to different particle loading behaviors. A particle loading curve shows the pressure drop as a function of particle loaded onto the filter media.

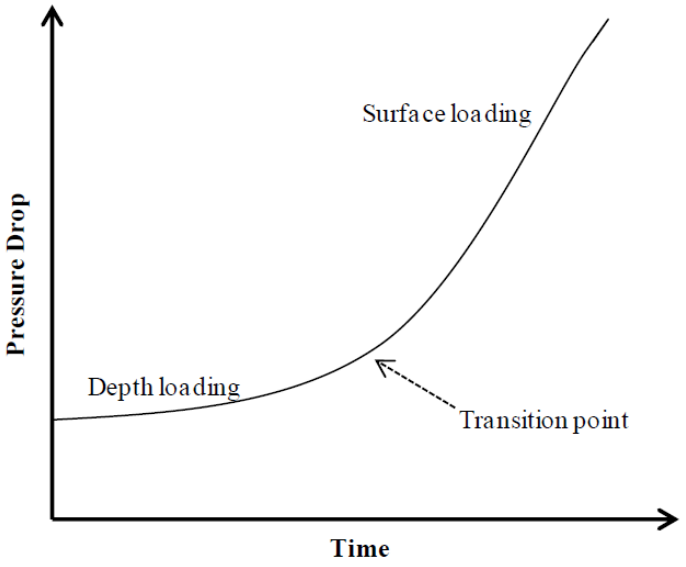

Figure 8. A particle loading curve which indicates increase in pressure drop across filter as a function of time, as more particulates are entrapped by the filter

A typical particle loading curve is shown in Figure 8. The curve has two distinct parts. The pressure drop increases slowly at the beginning and transitions into a phase with rapid increase in pressure drop. The slow initial increase in pressure drop is due to loading of particulates inside the depth of the media. Once the depth of the media is filled, the filter gets clogged and a filtrate cake is formed which acts as a surface filter. The filter cake results in higher pressure drop. The particle loading capacity of a filter can be increased by pleating the media. Generally, filters are used until it reaches the transition point between depth loading and surface loading as shown in Figure 8.

1.1.6 Non-woven media manufacturing

Fibrous filters media can be divided into two categories a) woven b) non-woven. Woven filter media have low voidage which creates high pressure drop. Also, these woven filter media, due to its low freeness, cannot be used in paper machine for large scale production. Non-woven media, on the other hand, is easier to manufacture on industrial scale due to high freeness,

and its ability to be calendared/compressed. Non-woven media has been used in the work discussed in this thesis. It can be prepared either through dry formed process or wet-laid process. Wet-laid process uses water as the medium, while dry formed process does not use any liquid. Commercially, non-woven media is prepared commercially from polymer using electrospinning and melt-blown processes. However, these technologies produce fragile structures that lack strength required for many applications. To overcome this problem, support fibers with 2-20 μm are used with nano-fibers layered over them. The problem with this kind of media is the 2-dimensional surface distribution of nanofibers. There is a necessity for developing non-woven media with 3-dimensional distribution of nanofibers, which is the focus of this thesis.

A non-woven media composed of carbon nanofibers was used in the work presented in this thesis. It was prepared using wet-laid process. The wet-laid process is similar to the wet-end of the paper making process. Wet-laid process was chosen because it can incorporate the existing method for nanofiber dispersion with wet-processing of microfibers. Aqueous slurry of fibers is prepared and poured through TAPPI sheet mold to make the non-woven filter media. The binding process used for the non-woven media is thermal binding (sintering). The fibers of the media are bonded by melting the surface of the fiber at high temperatures.

1.2 Focus Area

Small particle barrier filters are typically used to remove particulates below 2 μm. These filters are mostly used in conjunction with large particle continuous filter systems. The small particulate filters have high removal efficiencies; however, the fundamental limitation of these filters is their inability to hold higher amounts of dirt loadings. Since these filters do not possess higher dirt loading capacities, they have a relatively shorter useful capacity lives after which they yield an unacceptably high pressure drops. Also, in the ocean environment the salt aerosols are

highly concentrated with high mass fraction of 0.1 to 0.3 μm particulates, making small particle barrier filters a performance limiting element. Furthermore, new classes of high-speed vessels are expected to ingest even higher amounts of salt, further worsening the situation. Hence it is vital to develop better filters which can hold more dirt with lower levels of pressure drop and are potentially regenerable. These enhanced filter systems will contribute towards lowering M&O and replacement costs and increase the life and performance of various air breathing equipment.

To develop enhanced filter media, the first effort was on creating fibrous media of asymmetric porosity. Media with symmetric porosity utilizes sieving mechanism, resulting in cake formation on the surface of filter media and subsequent exponential increase in pressure drop. Conventional filters are surface filters which demonstrates this phenomenon, as shown in Figure 9a. To solve this problem, asymmetric 3-dimensional volume filters were synthesized in our lab, as shown in 9b. Wet-lay non-woven self-assembly technique is utilized to create such media. These volume filters have asymmetric porosity throughout the filter media.

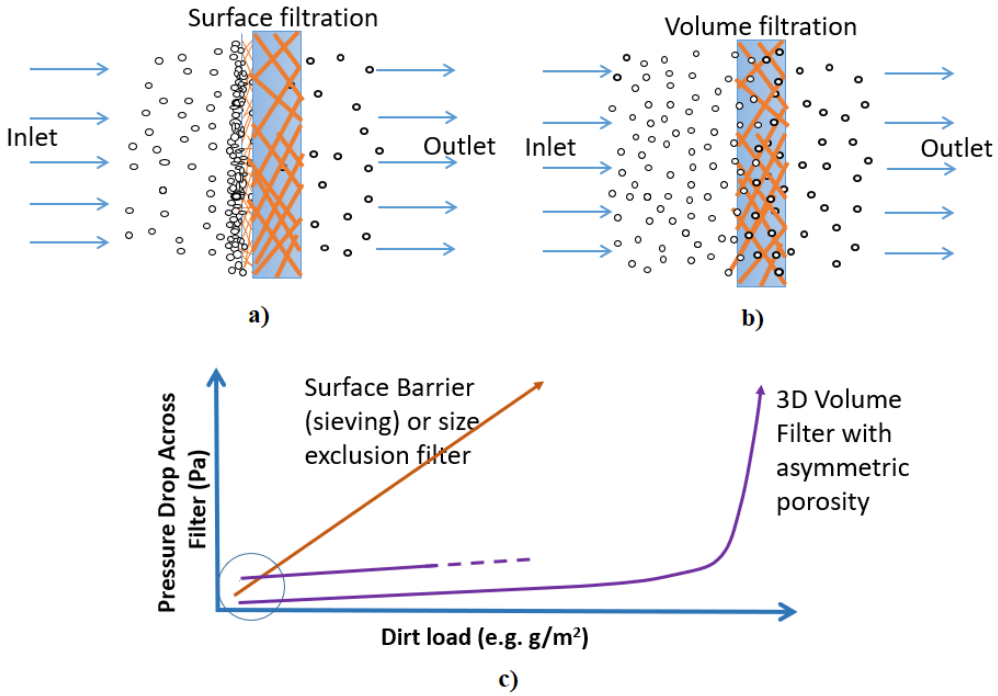

Figure 9. a) Surface filtration mechanism b) Volume filtration mechanism c) Pressure drop vs dirt load for surface filter and volume filter

Asymmetric porosity is created by using fibers of different length, diameter, composition and density. The asymmetry helps to significantly increase the particle loading before reaching unacceptable levels of pressure drop. The comparison of the filtration metrics between commercial GOTs filter and the 3-dimenional volume filter will be included in the subsequent chapters.

The following sections describe fundamental new strategies that was explored to further enhance the 3-dimensional volume filters for filtration of sea salt aerosols.

1.2.1 Incorporation of Nanofibers

The first hypothesis made for the work presented in this thesis is that the incorporation of nanofibers into the filter media enhances filtration of small particulates. The nanofibers will be placed into a 3-dimensional asymmetric structured media, to improve dirt holding capacity without unacceptable increase in pressure drop.

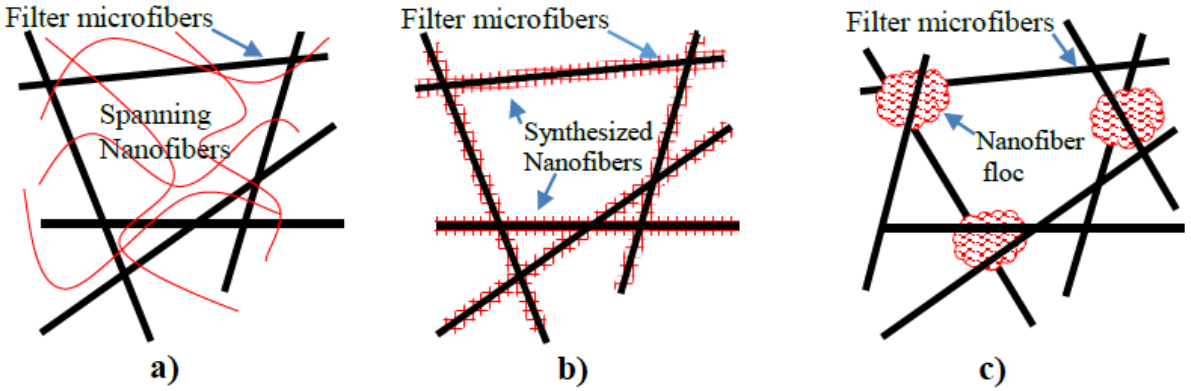

Figure 10. Different types of nanofibers inclusion a) Nanofibers that span the air stream b) “Fuzzy nanofibers” attached to larger structural fibers c) Nanofiber flocs embedded within microfiber medium

Nanofibers that contiguously span air flow opening, as seen in Figure 10a, creates an unusually high pressure drop.[7] This pressure drop results primarily due to the phenomenon known as “Form drag”. Form drag occurs as a result of small (sub-millimeter) opening size between the fibers.[8] Secondarily, the pressure drop also results due to air friction over the surface of fibers. Since there is a trade-off between the pressure drop and filtration efficiency, as indicated by Quality Factor metric, the effect of pressure drop can be minimized by improving the filtration efficiency. Smaller fibers with small diameter and higher surface area can remove particulates efficiently, thus potentially improving filtration efficiency and subsequently the Quality Factor. Hence, we proposed that using nanofiber flocs that do no contiguously span the filter space but are attached to larger structural fibers, as shown in Figure 10b and 10c, can potentially improve the filtration efficiency and Quality Factor.

Efforts have been made by our group previously by developing a filter media with carbon nano-structured synthesized within a sintered nickel microfibrous matrix. This idea is demonstrated in Figure 10b, where fuzzy nanofibers are carbon nanofibers developed over nickel microfibers. This sintered nickel microfibrous matrix with carbon nanostructures, as seen in Figure 11 was synthesized by thermal CCVD process via acetylene (C_2H_2) decomposition.[7] The disadvantage of this process was formation of amorphous carbon as a byproduct. In addition, a gradient of CNS growth from the surface to the centerline of media depth was discovered. Most importantly, the enhancement in filtration efficiency was only limited due to reduction in mean pore size of filter media, which counteracted the advantage of filtration enhancement due to wall slip over nanofibers.[7]

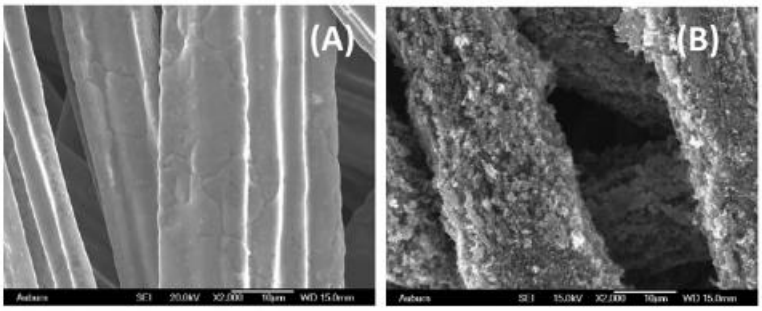

Figure 11. 12 μm SMM matrix a) before carbon nanofiber synthesis b) after nanofiber synthesis[7]

Some commercially available filters have electro-sprayed polymer nanofiber layer on top of larger diameter filter structure as shown in Figure 10a. However, these filters quickly retain a surface layer of entrapped particulates that form a filter cake. These filter cakes cause pressure drop across the media to increase significantly, beyond acceptable levels, rendering the filter unusable. This thesis includes evaluation of novel nano-floc embedded porous microfibrous filter media depicted in Figure 10c. These novel filter media were manufactured via wet-laid method using sheet mold and can be easily scaled up to industrial paper machines. The uniformity of nanofiber and nano-floc dispersion throughout the sheet has been established before.[9] Vapor Grown Carbon Fibers (VGCFs) produced by catalytic decomposition of hydrocarbon gases over nanocatalyst crystals were utilized to synthesize the nano-flocs.

1.2.2 Pore Volume of Activated Carbon Fiber for Salt Entrapment

The second hypothesis for work presented in this thesis is that the Activated Carbon Fibers (ACFs), which are porous in nature, can further enhance the particle loading capacity of filters because of its ability to wick salt aerosol into its pore. Due to the hydrophilic nature of ACFs and the capillary forces, ACFs containing media can entrap the salt aerosol inside the pores as shown in Figure 12. Salt particulates continuously load into wet pores, and this process pauses only after the water in pores dries out and the salt saturates. Hence water is believed to be the

fundamental driving force in this continuous salt aerosol loading into the activated carbon fiber pores.

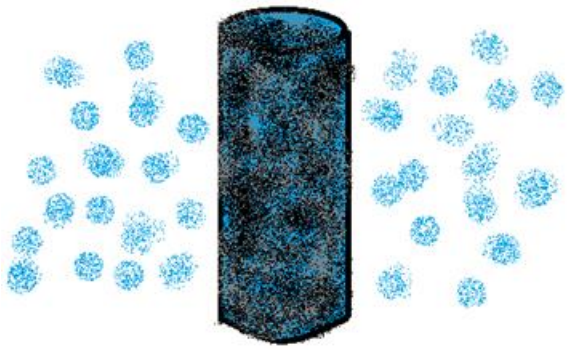

Figure 12. Salt aerosol being wicked into the porous activated carbon fiber

This hypothesis was tested by conducting particle loading experiment and plotting the particle loading curves. Amount of salt entrapped by different ACFs was also investigated. Further the adsorption phenomenon of water in activated carbon fibers was also studied and discussed in detail. The particle loading capacity of fibrous nano-floc filter media prepared in our lab were compared against the commercial GOTs media. The results are included in subsequent chapters.

1.2.3 Regeneration of Filter Media

The relative humidity (RH) at ocean environment is high (>72%). The sodium chloride is hygroscopic in nature and has a deliquescent point of 72%RH. Below the 72% RH, the salt particulates are in hydrated form and above 72%RH the salt particulates form aqueous droplets. This can potentially affect filtration performance parameters such as pressure drop, filtration efficiency, quality factor and particle holding capacity. Particularly, above 72%RH the salt water droplets could cause aqueous flooding. Hence the effect of hydrophobic Polytetrafluoroethylene (aka Teflon) to keep the water off the surface of filter is studied by coating nanofibrous filter media with PTFE. PTFE contains fluorine functional group and changes the surface chemistry of the surface fibers. When the water is kept off, the salt penetration into the media improves. Also, the

PTFE can potentially help with regeneration of filter media, prolonging filter lifetime. Experiments were performed and results are included in later chapters.

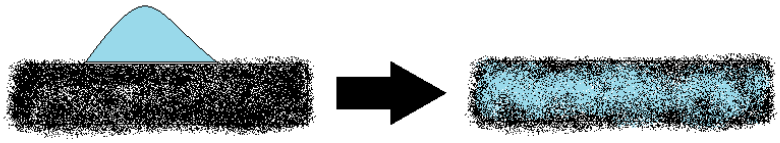

Water droplet being wicked into the pores of activated carbon fibers

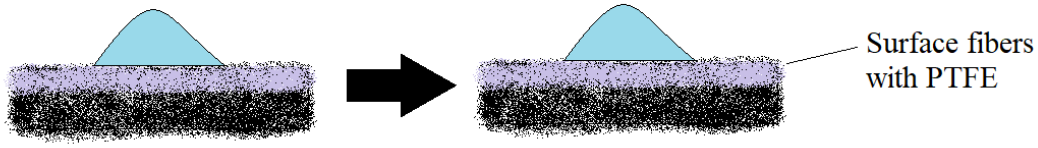

Water droplet beading up on the surface due to hydrophobic PTFE coating

Figure 13. Effect of PTFE coating on nano-floc filter media

Chapter 2: Novel Nanofiber Floc Embedded Filter Media's Performance and Evaluation

Using nanofibers with higher surface area has shown to have a significant enhancement in small particulate filtration.[7,9,10] These nanofibers when used in conjunction with structural microfibers can not only help reduce pressure drop across filter media but also increase the dirt holding capacity. Efforts have been made in our lab to create a 3D porous, asymmetric porous, non-woven filter media containing Activated Carbon Fibers (ACFs), Vapor Grown Carbon Fiber (VGCFs) and bi-component Polyester/Polyethylene Fibers. ACFs have shown great capability to remove particulates and gaseous contaminants simultaneously, hence it has been chosen as the main material for the development of this media.[1] In this study, these porous ACF nanofiber floc embedded filter media along with GOTs filter media were tested for evaluation of performance for salt particulate filtration, including pressure drop, filtration efficiency and quality factor.

2.1 AU Nano-floc Filter Media

AU Nano-floc embedded filters contain nano-sized flocs of VGCFs embedded inside polymer and activated carbon fibers. VGCFs are low cost nanofibers manufactured by catalytic decomposition of hydrocarbon gas over nanocatalyst crystals. Previous work by our lab have demonstrated increase in Quality Factor with optimal VGCF content of 1.4%.[1] As VGCF is increased more than 1.4%, the pressure drop across the filter media starts to increase significantly as shown in Figure 14. This was attributed to the reduction in mean pore diameter of the nano-floc media and the increase in total surface area because of entrapped VGCFs.[9]

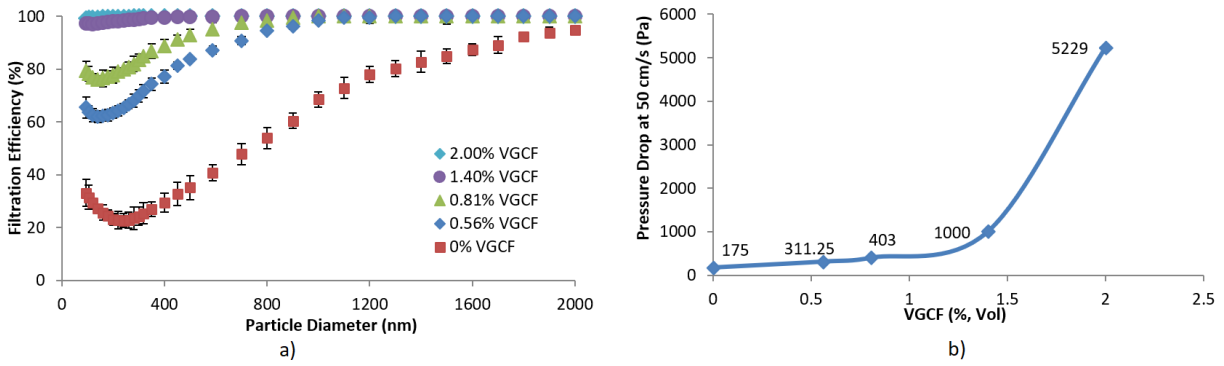

Figure 14. a) Filtration Efficiency b) Pressure drop curves of nano-floc media with different VGCF content[1]

These optimal amount of VGCFs (i.e. 1.4% vol) helps to change the conventional non-slip flow to slip flow, resulting in less flow resistance. In addition, slip flow makes air to flow much closer to fiber surface making it easier to entrap particulates, hence increasing filtration efficiency without anticipated pressure drop, as indicated by Quality Factor in Figure 15.[1]

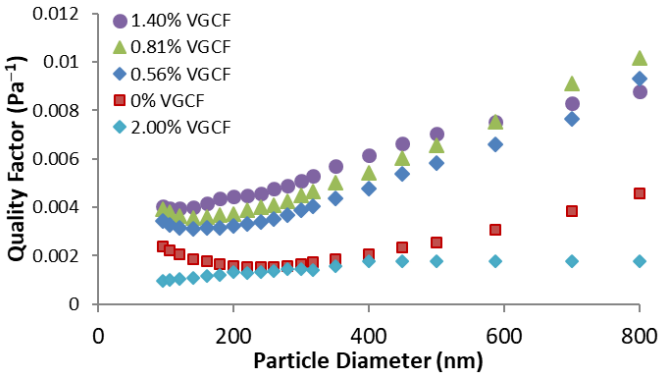

Figure 15. Quality Factor of nano-floc media with different VGCF content[1]

Slip flow occurs when air molecules encounter nanofibers with diameter that are on the order of the mean free path of air (65 nm at STP). During slip flow, the drag force per unit filter fiber surface area is lower than that of non-slip flow. At this condition the fluid mechanics boundary condition of zero velocity at the fiber surface does not hold true. Hence modification to the boundary condition is made in the form on non-zero velocity to include the molecular

movement of air. This new boundary condition is called the slip flow boundary condition. Slip flow effect becomes significant for fibers with diameters less than 500 nm.[9] The Knudsen number (Kn) is applied to describe the importance of molecular movement of air molecules at the fiber surface to the overall flow field.

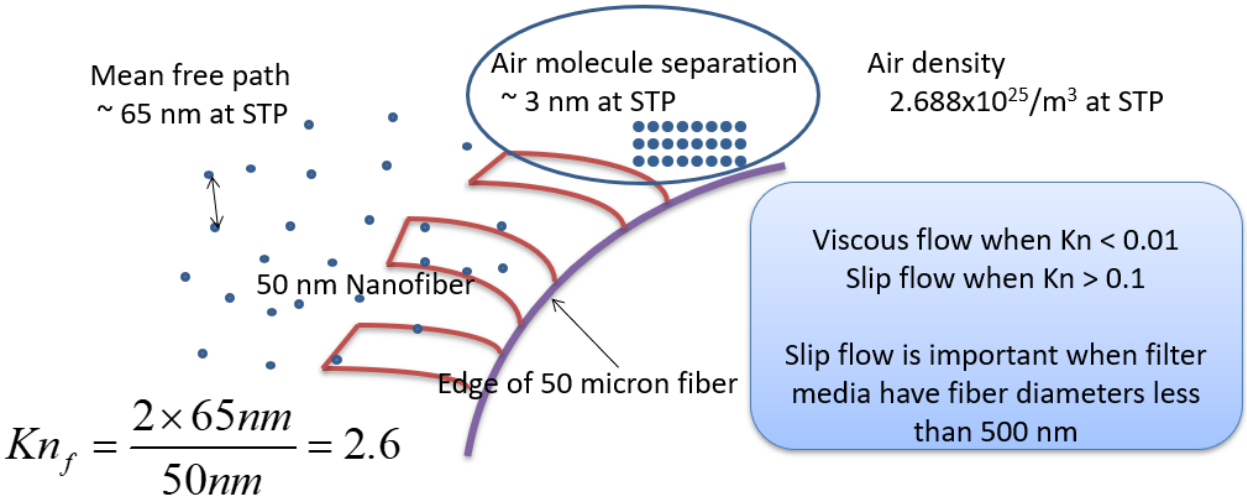

Figure 16. Slip flow phenomena in nano-fibers resulting due to nano-fiber inclusion

In addition, unlike commercial filters where nano fibers span entire air stream (Figure 17a) resulting in increased pressure drop, the VGCF nano-flocs do not span the entire air stream (Figure 17c). Hence the pressure drop increases relatively slowly in VGCF embedded media, contributing towards higher Quality Factor. Additionally, the VGCF nanofloc embedded media has high freeness, so it can be calendared/compressed. When the flocs get compressed the isolated flocs will be transformed to have a contiguous contact. Due to this characteristic, the nano-floc filtered can be easily manufactured in larger scale using traditional paper machine or sheet mold. However, the filters with spanning nanofibers cannot be used in paper machine since it has low freeness.

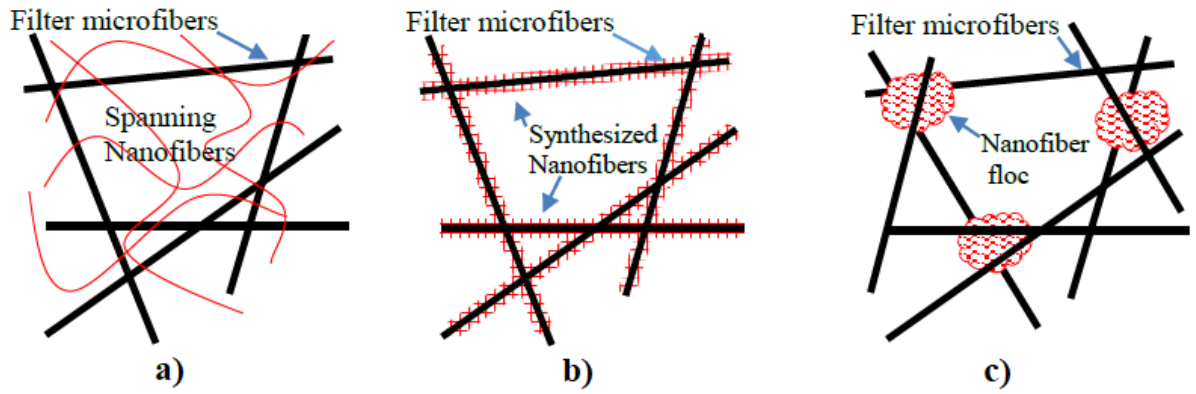

Figure 17. Different types of nanofibers inclusion a) Nanofibers that span the air stream b) "Fuzzy nanofibers" attached to larger structural fibers c) Nanofiber flocs embedded within microfiber medium

2.1.1 Materials Used to Fabricate AU Nano-floc Filter Media

ACFs with diameters 9-10 µm and length 3 mm were purchased from TOYOBO, Japan and Kynol, Japan. ACFs have shown great capability in removing particulates and gaseous contaminants. They are microporous fibers with large specific surface area ranging from 700 to 3000 m^2/g. They are made from synthetic fibers, like rayon or PAN, via a high-temperature carbonization and activation process.[4] Bi-component polyester/polyethylene fibers with diameter 13 µm and length 3-6 mm, used as binders for filter media, were obtained from KOSA. VGCFs with 150 nm diameter were purchased from Pyrograf Products Inc. Anionic surfactant Sodium Dodecyl Sulfate (SDS), and cationic surfactant Cetrimonium Bromide (CTAB) were purchased from Sigma Aldrich. FERAN-ICA Polymeric solution was used to disperse the polyester fibers and were obtained from Rudolf Group.

2.1.2 Synthesis of AU Nano-floc Filter Media

VGCFs have large Van-der Waals force and high surface energy between the fibers, resulting in fiber bundles. Hence to disperse, the VGCFs were first added in water, followed by

anionic surfactant SDS. The surfactant method of dispersing VGCF was chosen because of its ease of scalability and the inherent safety of the process. The suspension was agitated for 10 minutes using a stirrer. Partially dispersed VGCFs were then sonicated for 5 hours for complete dispersion. The dispersion occurred as a result of electrostatic repulsion created by the surfactant. Ultra-sonication was performed with an ultrasound processor from Fisher Scientific (Model # Solid State Ultrasonic FS-90) with time adjustments ranging from 0 to 30 minutes. The individual nano-fibers obtained after dispersion will not get entrapped within the microfiber matrix and will drain with water. Hence the solution for this problem was to flock the nano-fibers using cationic surfactant CTAB.

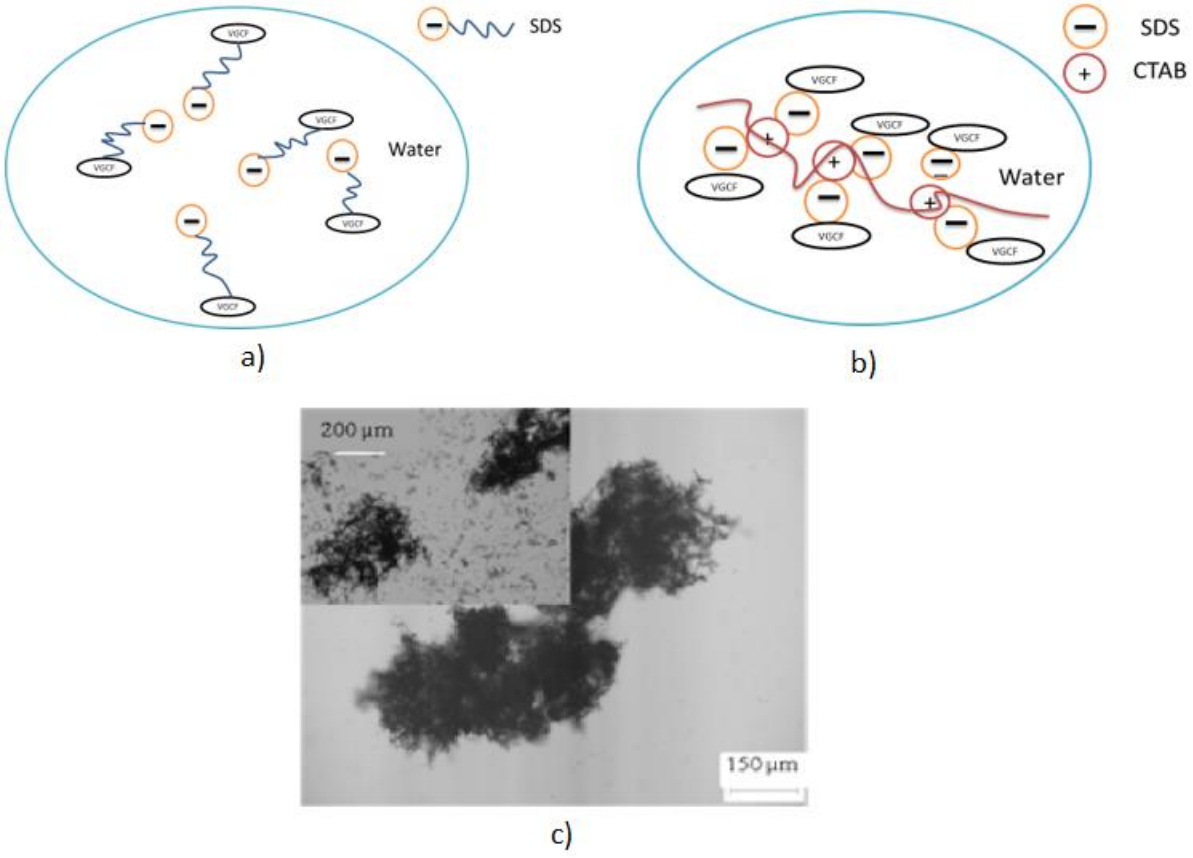

Figure 18. a) VGCF dispersion due to electrostatic repulsion created by SDS surfactant b) VGCF flocculation due to electrostatic attraction between positively charged CTAB and negatively charged VGCFs c) Optical microscope image of VGCF floc[9]

CTAB was added, in presence of agitation, to create small nano-flocs of VGCFs. The formation of the nano-flocs was due to the electrostatic attraction between negatively charged VGCFs and positively charged CTAB surfactant. After VGCF flocking, the density of VGCFs decreased from 0.0272 g/cm^3 (as-received) to 0.0022 g/cm^3. The VGCF suspension was left in quiescent state overnight before using in the wet-laid process.

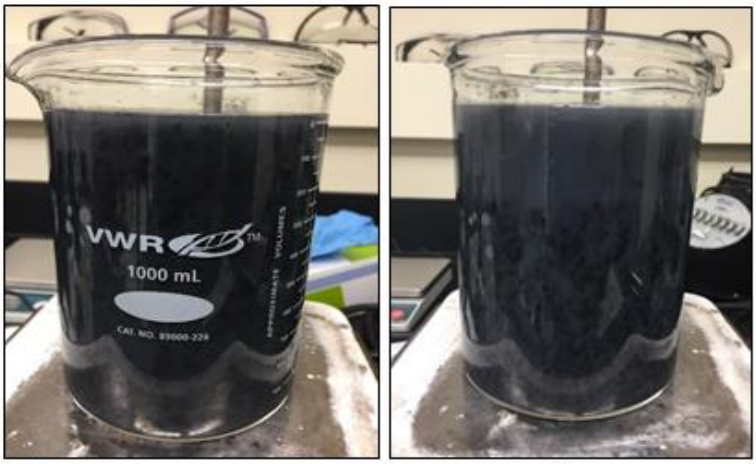

Figure 19. a) VGCF suspension before nano-floc formation b) VGCF suspension illustrating nano-flocs formed

Next, the ACFs were dispersed in water using a blender. Due to the lack of hydrogen and oxygen in ACFs, it is impossible to form a strong media via hydrogen bonding. Thus bi-component polyester/polyethylene fibers were used as binders. The bonding would be created as a result of melting of the polyester fibers. FERAN-ICA polymeric solution was employed as a dispersing agent for the polyester fiber. The mixture of ACFs and polyester fiber was combined with the VGCF suspension and were transferred into a 16cm diameter TAPPI hand-sheet former.

This dispersion of nano and microfibers are then rapidly filtered over a wire mesh. The rapid drainage of water creates a stack of randomly oriented microfibers called the preform. Water was drained from the preform using a hand roller followed by drying at 140°C in air for 15-20 mins. The drying process also melts the polyester/polyethylene fibers to create a strong bonded media. Finally, the samples used were punched out from 200 cm^2 sheet using a circular steel punch. Each sample was 1.03 in diameter with a thickness of ca. 3.2mm.

Figure 20. Wet-laid process of synthesizing AU Nano-floc filter media[1]

2.2 Nomenclature of Samples Prepared

The samples prepared for this project, using wet-laid method mentioned above are tabulated in the table below:

		Composition of Sample (200 cm^2 sheet)			

Sample Number	**Sample Name**	**Bicomponent (Polyester/Polyethylene) Fiber (g)** 13 µm diameter	**Activated Carbon (g)** 9-10 µm diameter	**Surface Area of ACF (m^2/g)**	**VGCF (g)**
1	AU Kynol 1000 Cloth Nano-floc filter	2	4	1000	0.75
2	AU Kynol 1000 Felt Nano-floc filter	2	4	1000	0.75
3	AU Toyobo 1600 Cloth Nano-floc filter	2	4	1600	0.75
4	AU Toyobo 2500 Fiber Nano-floc filter	2	4	2500	0.75
5	Donaldson (Used)	NA	NA	NA	NA
6	Donaldson (Ultra-sonicated Clean)	NA	NA	NA	NA

Table 1. Nomenclature of different filter media and its composition

Donaldson (Used) and Donaldson (Ultra-sonicated Clean) are samples punched out of industrial air filter cassette used by Navy in LCAC, manufactured by Donaldson Inc. Donaldson (Used) was used in the same condition as it was received. However, Donaldson (Ultrasonicated Clean) was cleaned in water by applying ultra-sonication. Samples 1-4, prepared in our lab, vary in type of activated carbon fiber and the amount of polymer and VGCF used.

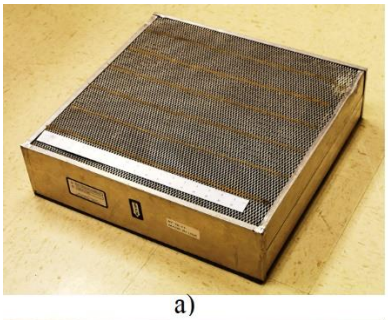

a)

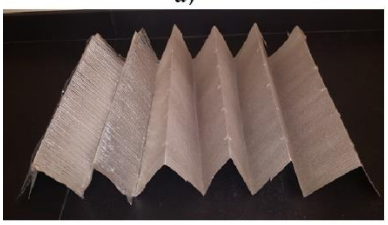

b)

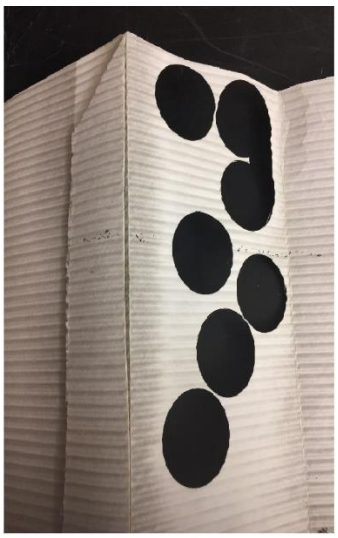

c)

Figure 21. a) Donaldson filter cassette b) Pleated Donaldson filter media obtained from the filter cassette c) Samples cut out of the Donaldson filter media

2.3 Experimental Setup

2.3.1 Bench-Scale Filtration Setup

The experimental setup used for testing the performance of different filter media for salt particulate filtration is shown in Figure 22. Compressed air was passed through the desiccant containing silica gels to remove the moisture, followed by High Efficiency Particulate Air (HEPA) filter to get rid of any contaminants. Out of the two streams flowing through the process, the first is the nebulizing air stream. The nebulizing air stream was used to generate aerosol with salt particulates. The flow rate of nebulizing air was controlled using a mass flow controller. Sodium chloride (NaCl) solution (5% [w/w]) was used in all experiments. Hudson RCI micro mist nebulizer from Teleflex Medical was used to generate the salt aerosol. The wet aerosol was dried by passing it through a diffusion dryer (DD 250) manufactured by Air Techniques International. Aerosol neutralizer (Model-9000) by Brechtel and two Polonium-210 strips by NRD, LLC were used to neutralize the static charges developed due to aerosolizing. A second stream of air was mixed with the neutralized salt aerosol to dilute it, to ensure that the concentration of salt particle did nor exceed the limit of particle counter. The diluted salt aerosol was passed through the filtration section. The filtration section consisted of two stainless steel pipes (1in ID) attached by two flanges. The filter media was placed in between the two pipes and sealed with foam gaskets. The pressure drop across the filter media was recorded using a pressure transducer by Omega. The filtration efficiency was calculated by using the particle count data recorded by Laser Aerosol Spectrometer (LAS-XII) from TSI.

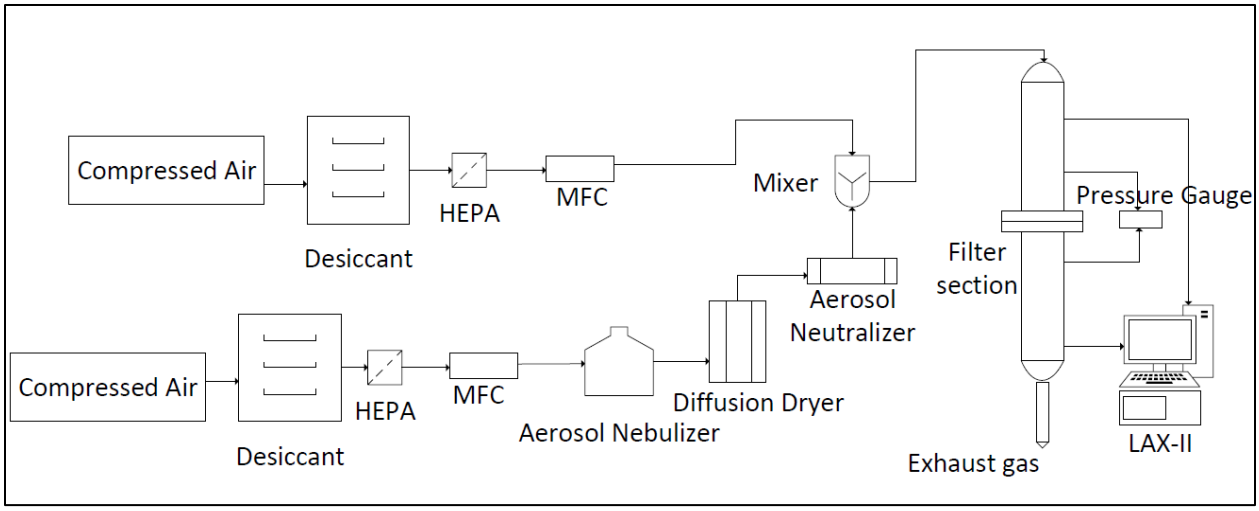

Figure 22. Bench-scale experimental setup for salt particulate filtration

The sampling process was initialized by taking a 60 second sample count from the upstream isokinetic probe. In order to take both upstream and downstream sample without moving the spectrometer, a three-way valve was then switched to take a sample from the downstream isokinetic probe. The spectrometer then measured a 60 second count of the downstream particles. For each test, eight samples for both upstream and downstream were collected. Error bars for 95% confidence interval are reported in the filtration efficiency data as per the ASHRAE 52.2 Standard. However, for each test, the first few samples were always not very accurate due to the residue particles remaining in the sampling probes from previous runs. Therefore, before each test, a pre-cleaning procedure was carried out by purging pure air into the whole system.

2.3.2 Generation of Aerosol Particulates

Aerosol particulates were generated using nebulizer by Hudson RCI Micro Mist Nebulizer by Teleflex Medical, USA. 5% NaCl solution was used to generate the salt aerosol particulates. Since there is an upper limit on the amount of salt aerosol that the LAS-XII particle counter can sample, the Hudson nebulizer was chosen because it operated within the limit.

Figure 23. Hudson RCI Micro Mist Nebulizer

It is important to determine the concentration of salt particle generated by Hudson Nebulizer. The salt concentration can be calculated in parts per million by weight (ppmw), and can be calculated with equation 5, where c_{salt} is the concentration of salt in ppmw, m_{salt} is the mass of sea salt (g) and m_{air} is the mass of air (g).

$$c_{salt} = \frac{m_{salt}}{m_{air}} * 10^6 \qquad Equation\ 5$$

Donaldson media was used as a filter media. It was assumed that all particles would be captured when the media was clogged. The difference in the mass of clogged media and clean media would give the mass of salt particulates captured from the upstream. This mass was calculated as $m_{salt} = 8.34 \times 10^{-3}$ g. The total volume of air during mass increase was 324 liters at 53.2 cm/s within 20 mins. Hence the salt concentration in the aerosol upstream was calculated as

$$c_{salt} \approx \frac{8.34*10^{-3}}{(324/22.4)*29} (* 10^6) = 19.8 \text{ ppmw}$$

2.3.3 LAS-XII Airborne Particle Spectrometer

LAS-XII Airborne Particle Spectrometer was used to count the number of particulates upstream and downstream of the filter media. This data was then used to evaluate filtration efficiency. LAS-XII is a high sensitivity laser particle size spectrometer designed for sampling and counting airborne particulates from 90 nm to 7.5 µm. The spectrometer is operated via a built-in computer utilizing Windows XP operating system to run the interface for instrument control, data

display, recording and output. It uses Helium-Neon (He-Ne) as laser source. Air flow rate can be set between 10-100 sccm.

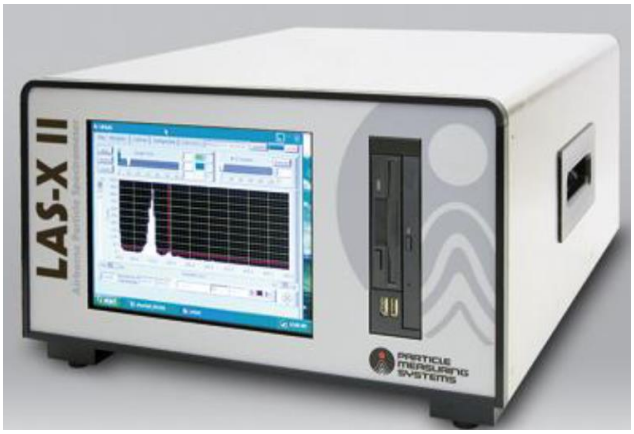

Figure 24. Laser Airborne Spectrometer manufactured by Particle Measuring Systems Inc.

LAS-XII operates on the principle that the light scattered by a particle within an active laser cavity is a direct function of its size. Particles produce pulses of light during transit through the laser beam. The light pulses are sensed by a pair of detectors that in turn are analyzed by four cascading amplifier stages coupled to analog-to-digital converters for sizing. Particles are aerodynamically focused to a sample stream diameter smaller than the laser beam diameter in order to avoid edge effects. The particle range spanned by LAS-XII is from 0.09 to 7.5 μm and particle data are binned into up to 100 user defined size channels.[14]

2.3.4 Test Conditions

Mass flow controllers were adjusted to get aerosol face velocity of 53.2 cm/s, throughout all experiments mentioned in this chapter. The RH of the salt aerosol was 2-4%. The concentration of salt particles was around 73,000 per 50 cm^3 of air with 1460 particles per cm^3 of air.

2.4 Performance Metrics Used to Evaluate Filter Media

2.4.1 Filtration Efficiency

The filtration efficiency is the most important metric used to measure the performance of a filter. It primarily depends on type of filter media used. It also depends on particle size of filtrate, filtration area and filtration velocity. The average filtration efficiency was evaluated using equation 6, according to ASHRAE 52.2 Standard[17]. It is expressed as a number between 0 and 1. For each filter media, 8 runs of sampling was performed upstream and downstream for 30 seconds per sampling.

$$E = \left(\frac{n_{up} - n_{down}}{n_{up}}\right) \qquad Equation\ 6$$

2.4.2 Quality Factor

Higher filtration efficiency typically indicates larger pressure drop for a filter. There is a tradeoff between filtration efficiency and pressure drop. To deal with this phenomenon, a new term Quality Factor (QF) was defined to measure whether the increase in pressure drop is warranted by the increase in filtration efficiency.[4,5] It is calculated as the ratio of fraction capture per unit thickness to the pressure drop per unit thickness.[3]

$$QF = -\frac{\ln(1 - E)}{\Delta P} \qquad Equation\ 7$$

According to equation 7, the larger filtration efficiency and smaller pressure drop leads to higher quality factor. The filtration efficiency plays more significant role compared to pressure drop because of the logarithm.

2.5 Results

2.5.1 Pressure Drop vs Face Velocity

Pressure drop corresponds directly to the energy consumption as it is indicative of the work done by pushing air through the filter.[11,18] Higher pressure drop across a filter media causes

more energy to be expended to push air through it. Hence, it is critical to consider pressure drop as a performance metric to evaluate filter media.

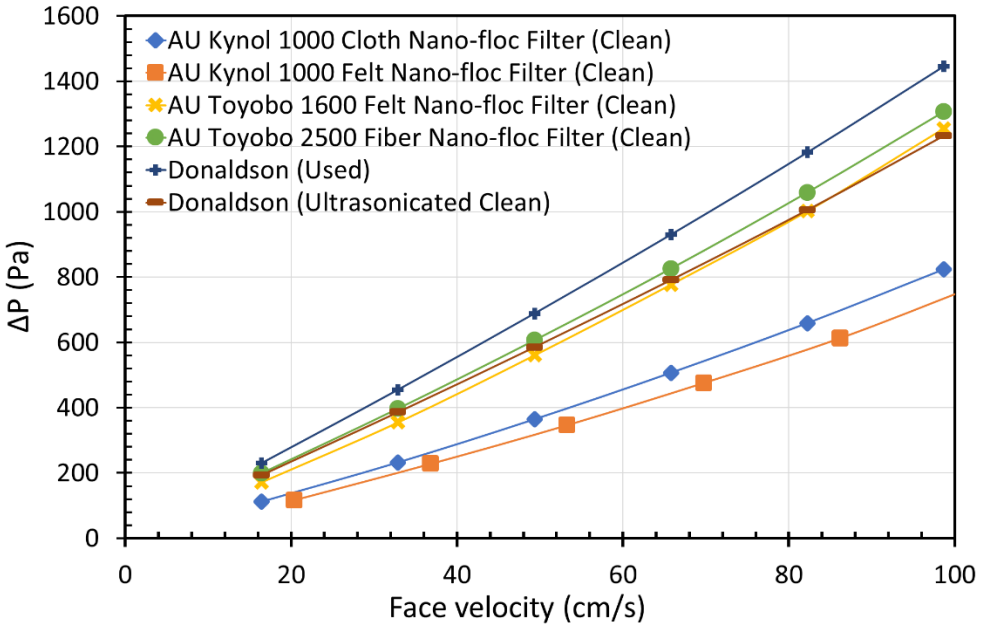

Figure 25. Pressure drop across different filter samples with respect to face velocity

Pressure drop across samples listed in Table 1 were measured at varying face velocities of air passing through it. The pressure drop values across the media was recorded by a pressure transducer by Omega. All filter media show a general trend of increasing pressure drop, as the face velocity value of the air through it increases. This is due to increased resistance for the flow produced by fibers at higher velocities. However, for a constant value of face velocity, different media registered different pressure drop values. Figure 25 shows that at a constant value of face velocity, the Donaldson (Used) sample had the highest pressure drop across it. However, the Donaldson (Ultrasonicated clean) sample had similar pressure drop values across it, as the samples AU Toyobo 1600 Felt and AU Toyobo 2500 Fiber Nano-floc Filters prepared in our lab. AU Kynol 1000 Cloth and AU Kynol 1000 Felt Nano-floc Filters, prepared in our lab, had significantly lower pressure drop values across it, compared to the Donaldson (Ultrasonicated clean) sample. This

indicates that AU Kynol 1000 Cloth and AU Kynol 1000 Felt Nano-floc Filters consume less power to operate compared to the Donaldson (Ultrasonicated clean) GOTs sample. The higher pressure drop across Donaldson media can also be attributed to the combined effect of non-homogeneous pore structure, non-porous nature of the fibers and the surface filtration mechanism employed by Donaldson media.

2.5.2 Salt Particulate Filtration Efficiency and Quality Factor Results

LAS-XII spectrometer was used to measure the count of particles before and after the filter media. There is a point with lowest filtration efficiency, in the region between 40 nm and 400 nm where none of the filtration mechanism is strong enough to capture the particles. This is called the Most Penetrating Particle Size (MPPS). For particles with size smaller than MPPS, the dominant filtration mechanism is diffusion, whereas for particles with size bigger than MMPS, the dominant filtration mechanism is inertial impaction. Below the MPPS, i.e. in the diffusion dominant region, the filtration efficiency increases with decrease in particle size. Above the MPPS, i.e. in the inertial impaction region, the filtration efficiency increases with increase in particle size. Where the MPPS lies depends on the face velocity of air. Higher the face velocity of air, the lower the MPPS[3].

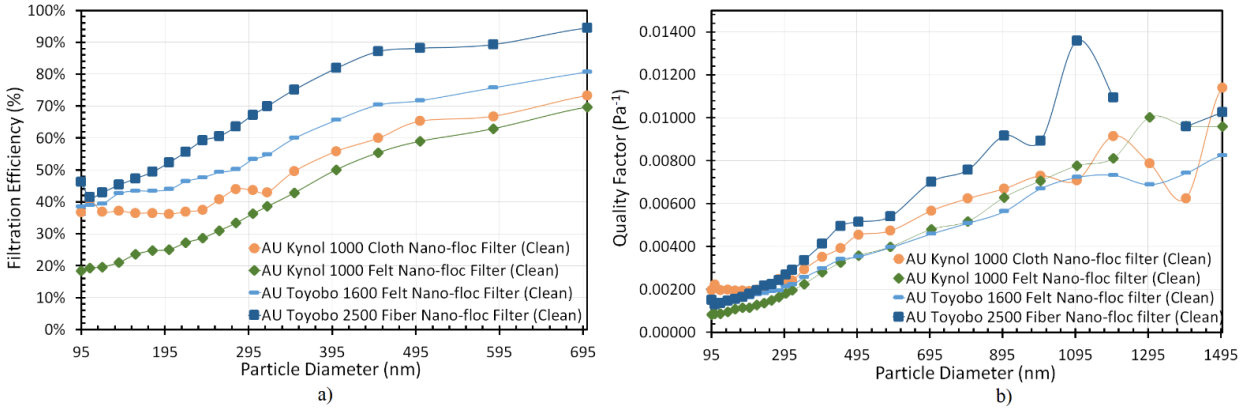

Figure 26. a) Filtration Efficiency b) Quality Factor for Different Filter Media at 0 g/m^2 Salt Loading. Flow rate 50 cm/s and RH 2-4%

From Figure 26a, MPPS cannot be seen in the 95 nm to 700 nm particle diameter range. Hence it is evident that the MPPS must be below the 95 nm particle diameter size. LAS-XII cannot detect particulates below 95 nm. Hence all the data presented in Figure 26 is from the inertial impaction region. As the particle size increases, the filtration efficiency goes up because bigger particles are more likely to be captured by the fibers. This trend can be seen in Figure 26a, for all filter media studied. Regarding different filter media studied, the filtration efficiency of AU Toyobo 2500 Fiber Nano-floc Filter was found to be the highest across the entire particle diameter range. This can be attributed to larger surface area of activated carbon fiber with 2500 m^2/g being able to accommodate more particulates compared to other media with relatively smaller surface area fibers. As the surface area of the fiber decreased, so did the filtration efficiency. The AU Kynol 1000 Felt Nano-floc Filter showed significantly lower filtration efficiency compared to the AU Toyobo 2500 Fiber Nano-floc Filter, for a constant value of particle diameter.

The Quality Factor additionally accounts for pressure drop associated with increase in filtration efficiency. The higher the Quality Factor, the better the filter performance. As seen in Figure 26b, for the particles with diameter above 300 nm, the Quality Factor for AU Toyobo 2500 Fiber Nano-floc Filter had the highest quality factor. It means that the AU Toyobo 2500 Fiber Nano-floc Filter can withhold significant amount of particles without large increase in pressure drop. Below 300 nm, AU Kynol 1000 Cloth Nano-floc Filter showed a slightly better quality factor. Hence it can be concluded that for particles below 300 nm diameter, the AU Toyobo 2500 showed marginal increase in pressure drop compared to AU Kynol 1000 Cloth Nano-floc Filter media. However, these parameters could change as the salt particles keep loading into the filter

media. Hence further tests were performed to study the evolution of filtration efficiency and quality factor at higher particle loading.

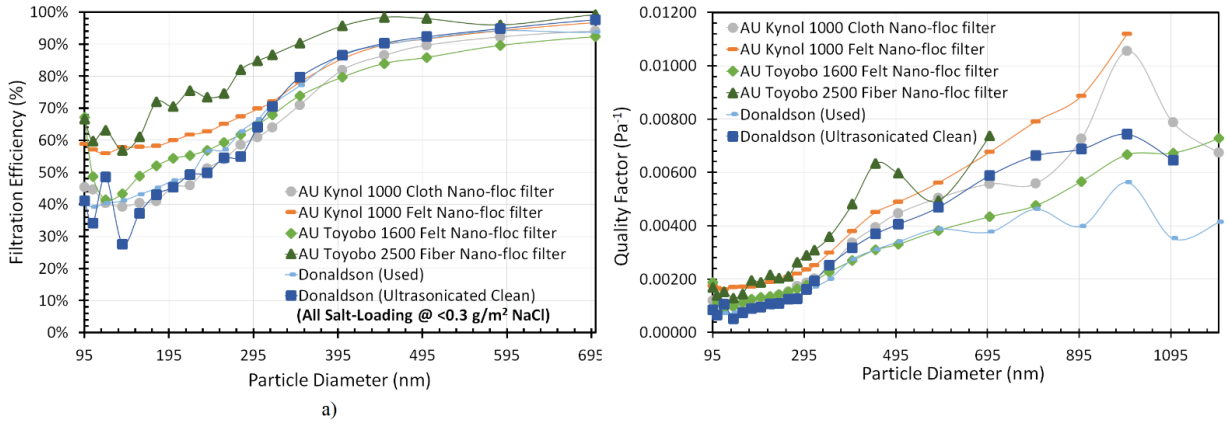

Figure 27. a) Filtration Efficiency b) Quality Factor for Different Filter Media at <0.3 gm/m^2 Salt Loading. Flow rate 50 cm/s and RH 2-4%

Same samples were continued to load with more salt particulates till it reached 0.3 g/m^2 NaCl loading. MPPS for AU Toyobo 2500 Fiber, AU Kynol 1000 Cloth and Donaldson (Ultrasonicated Clean filter media were seen at 140 nm particle diameter. At this particle size, none of the filtration mechanism is strong enough to hold the particle. Below 140 nm, the dominant mechanism is diffusion, and filtration efficiency increases with decreasing particle size. Above 140 nm, the dominant filtration mechanism is inertial impaction, and filtration efficiency beyond this point increases with particle diameter, as shown in Figure 27a. Similarly, MPPS for AU Kynol 1000 Felt and AU Toyobo 1600 Felt Nano-floc filter media were seen at 120 nm. However, the MPPS for Donaldson (Used) filter media could not be seen in the 95 nm to 700 nm particle diameter range. Regarding filtration efficiency, the AU Toyobo 2500 Fiber Nano-floc filter still demonstrated the highest filtration efficiency at 0.3 g/m2 loading, up to 600 nm particle diameter. The commercial Donaldson (Ultrasonicated Clean) had significantly lower filtration efficiency up to 600 nm. The Donaldson filter media is a much thinner media (ca. 0.4 mm) compared to the

nano-floc media (ca. 3.2 mm) synthesized in our lab. The Donaldson media utilizes surface filtration mechanism, since it does not have any depth to it. In Donaldson filter, the salt particulates keep loading directly onto the surface until a filtrate cake is formed, yielding unusually high pressure drop. In addition, the Donaldson media does not have homogeneous pore structure throughout the media, which further contributes towards faster increase in pressure drop. However, the nano-floc media developed in our lab uses volume filtration in addition to surface filtration mechanism. The pores in the depth of the media get filled up with salt particulates and once the depth is completely saturated with salt, the surface filtration begins. Thus, the nano-floc media can hold significantly higher amount of salt particulates compared to Donaldson filter media. Also, the homogeneous pore structure throughout nano-floc media contributes in lowering pressure drop, compared to surface filters. The AU Toyobo 2500 Fiber Nano-floc filter showed better filtration performance due to larger surface area of Toyobo 2500 fibers. Larger surface area provides the opportunity for fibers to hold more particulates. AU Kynol 1000 Felt and AU Toyobo 1600 Felt Nano-floc filter media also had higher filtration efficiency compared to Donaldson (Ultrasonicated Clean) filter media up to particle diameter of 300 nm. The activated carbon fibers are porous in nature and can entrap salt particulates inside the pores as well, unlike the Donaldson filter media which is most likely made of non-porous polymer fibers.

Similarly, the Quality Factor for AU Toyobo 2500 Fiber Nano-floc filter was found to be higher for particle diameter up to 700 nm, compared to any other media. It can be attributed to the large surface area and porous nature of Toyobo 2500 fibers, contributing towards holding more salt particulates without unacceptable increase in pressure drop. AU Kynol 1000 Felt also demonstrated better Quality Factor compared to commercial Donaldson (Ultrasonicated Clean) sample. This means that the increased pressure drop for AU Toyobo 2500 Fiber and AU Kynol

1000 Felt Nano-floc filters are warranted by increase in filtration efficiency. This further validates that the inclusion of nano-flocs into filter media improves filtration performance significantly.

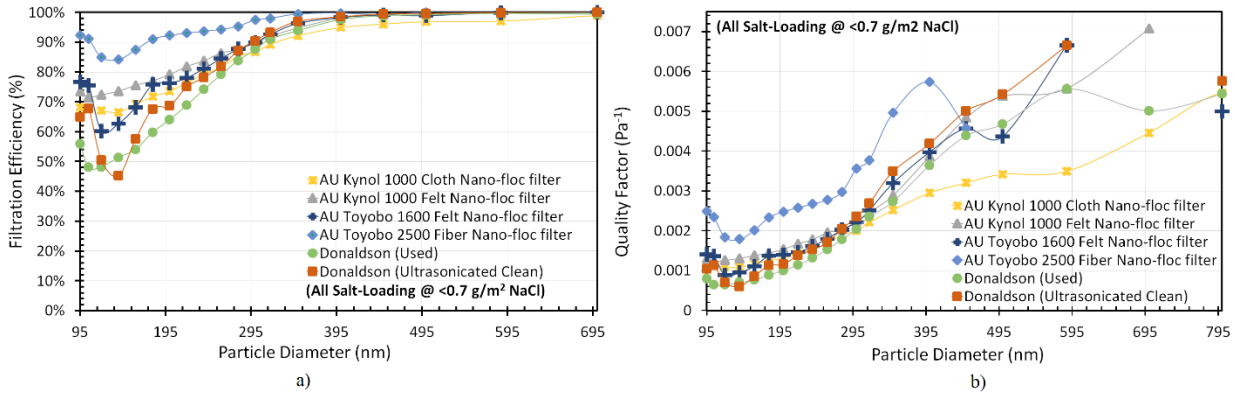

Figure 28. Filtration Efficiency and Quality Factor for Different Filter Media at <0.3 gm/m^2 Salt Loading. Flow rate 50 cm/s and RH 2-4%

Further loading of salt particulates were performed till a loading value of ~0.7 g/m2 NaCl was recorded. The filtration efficiency at this level of loading still indicated AU Toyobo 2500 Fiber Nano-floc media to be superior compared to other filter media up to 400 nm particle diameter, as shown in Figure 28a. Up to 260 nm particle diameter, all other samples demonstrated higher filtration efficiency compared to commercial Donaldson (Ultrasonicated clean) sample. This is due to the porous nature and large surface area of activated carbon fibers used in Nano-floc filters which enable them to entrap more salt particulates.

Similarly, the Quality Factor was also obtained for all filter media. As shown in Figure 28b, the AU Toyobo 2500 Fiber Nano-floc filter media had significantly higher quality factor compared to other filter media, particularly up to 400 nm particle diameter. This indicates that the increase in pressure drop for AU Toyobo 2500 Fiber Nano-floc filter media is warranted by the high filtration efficiency. The lower pressure drop across these nano-floc filters is also due to nano-flocs which do not span the entire flow stream, and due to the homogeneous pore structure of nano-

floc filter media. This creates less resistance to the flow. The other media had relatively similar quality factor. This further validates the fact that using high nano fibers with high surface area and porosity during filter manufacturing can increase dirt holding capacity and increase the lifetime of filter. This also contributes towards lowering costs associated with purchasing new filters and maintenance.

2.5.3 SEM Images

SEM images were obtained for different filter media samples, which contain surface morphology, image contrast and surface topography. SEM were performed before and after loading the salt particulates into the filter media.

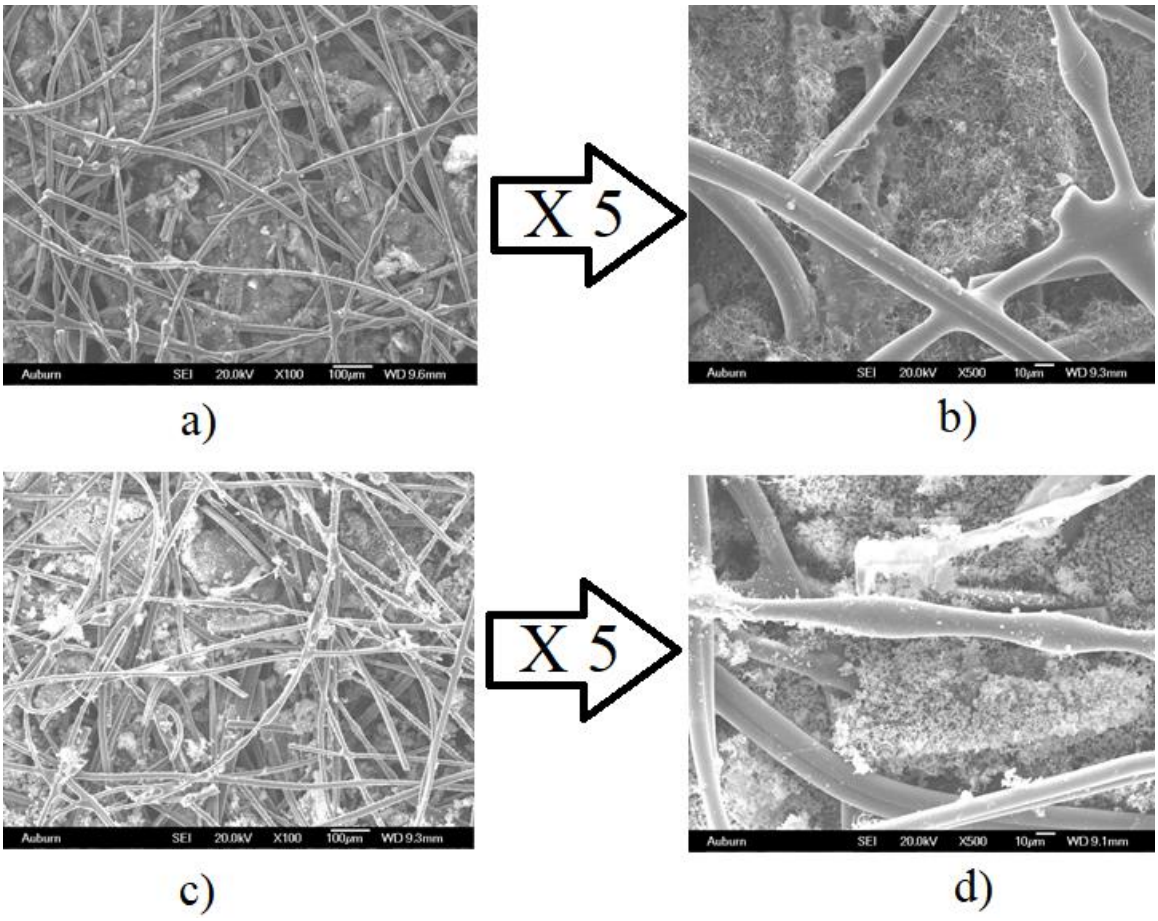

Figure 29. SEM images of the AU Toyobo 1600 Felt Nano-floc filter (a, b) before loading NaCl (c, d) after loading NaCl (39.4 g/m^2 at 6284 Pa)

Figure 29a shows a uniform distribution of bi-component polyester/polyethylene fiber and activated carbon fiber in the AU Toyobo 1600 Felt Nano-floc filter media. Figure 29b is the magnified version which shows that the bi-component polyester/polyethylene fiber have melted and formed a strong bond to hold the VGCCF flocs. Figure 29c shows the AU Toyobo 1600 Felt Nano-floc filter media after loading the salt particulates. Figure 29d, the magnified version, shows that the salt particulates are efficiently entrapped by the VGCF nano-flocs. The homogeneous pore structure of the filter media can also be seen.

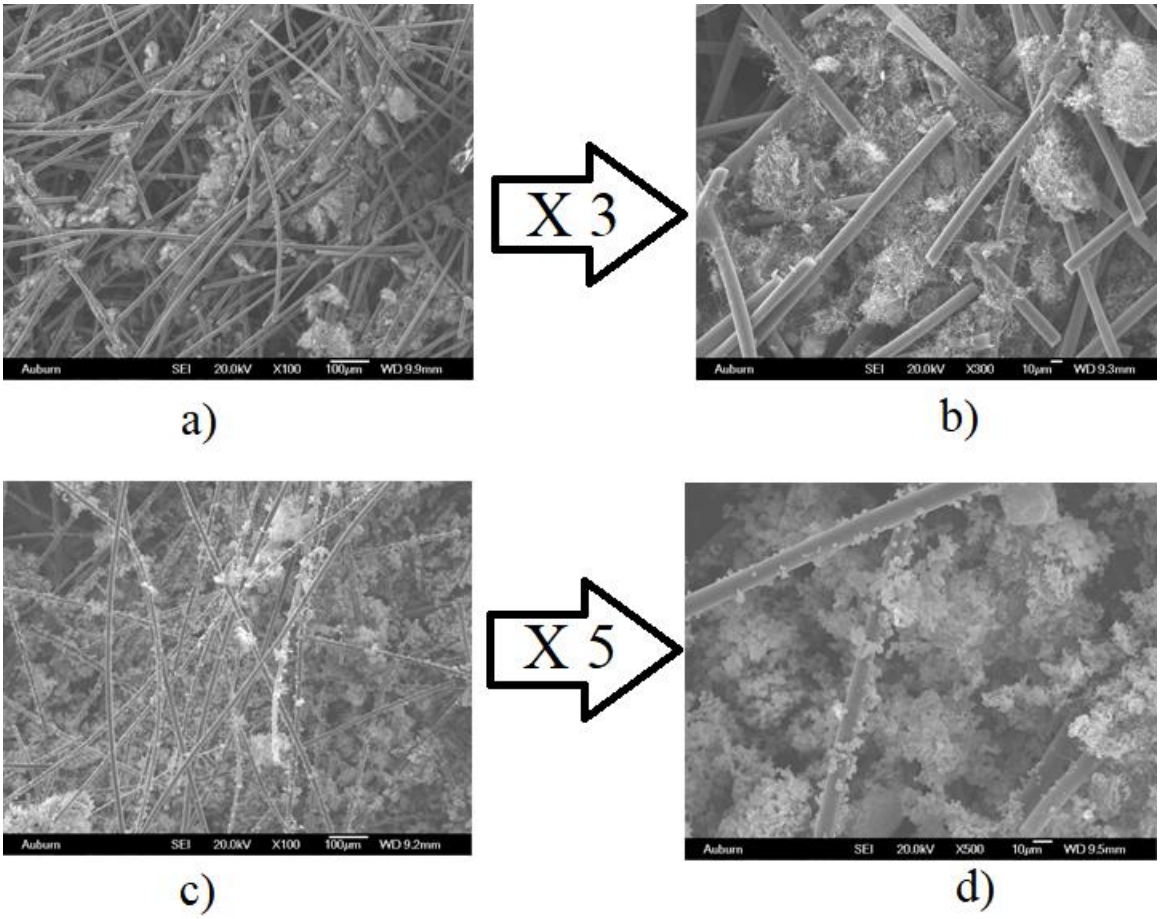

Figure 30. SEM images of the AU Toyobo 2500 Fiber Nano-floc filter (a, b) before loading NaCl (c, d) after loading NaCl (15.8 g/m^2 under ca. 4.9% RH)

Figure 30a also shows a uniform distribution of bi-component polyester/polyethylene fiber, activated carbon fiber and VGCF nano-flocs in the AU Toyobo 2500 Fiber Nano-floc filter

media. The VGCF nano-flocs is clearly seen to be distributed between the bi-component fiber and activated carbon fiber. Figure 30b is the magnified version, which shows a homogeneous pore structure of the filter media. Figure 30c shows the AU Toyobo 2500 Fiber Nano-floc filter media after loading the salt particulates. Figure 30d, the magnified version, shows that the salt particulates are efficiently entrapped by the VGCF nano-flocs. Additionally, it also shows the salt particulates are trapped better around the bi-component and activated carbon fibers compared to the AU Toyobo 1600 Felt Nano-floc filter media.

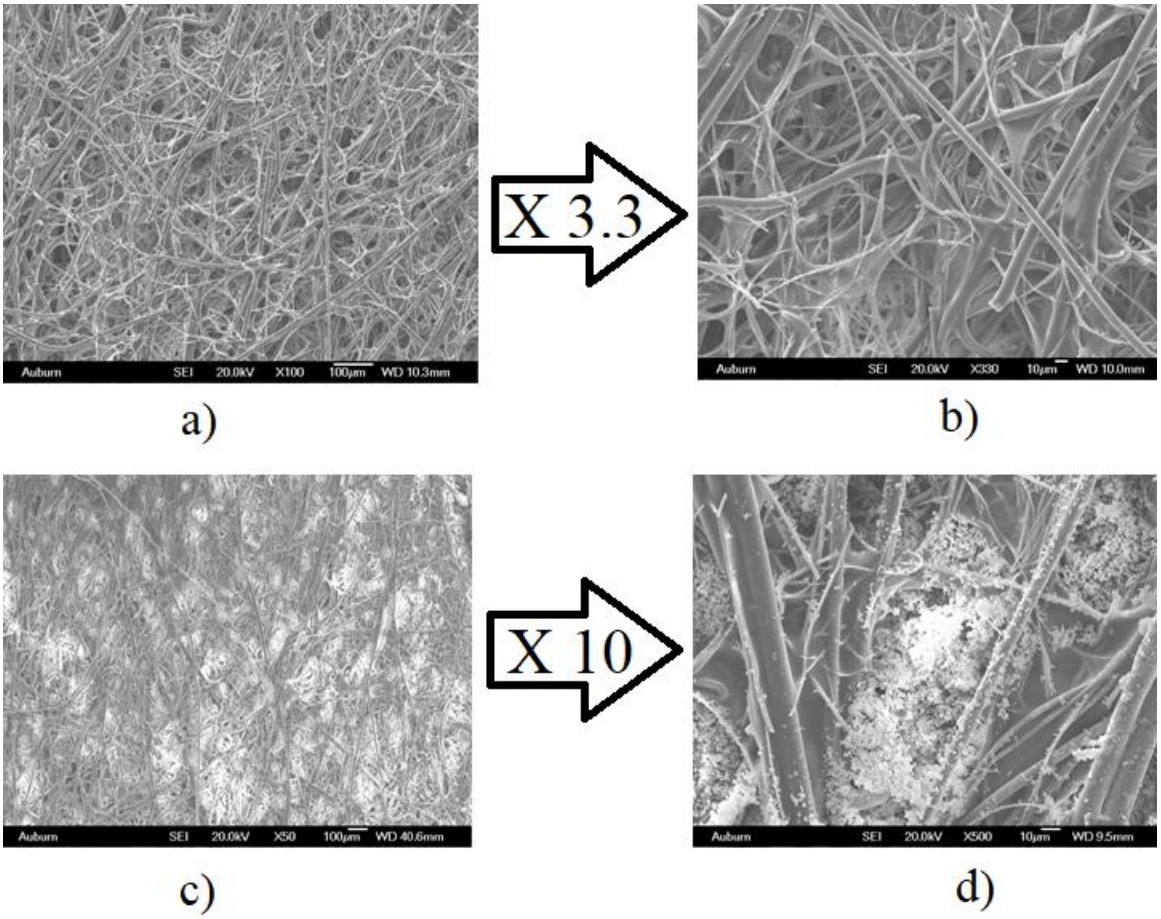

Figure 31. SEM images of the Donaldson (Ultrasonicated Clean) (a, b) before loading NaCl (c, d) after loading NaCl (5.9 g/m^2 at a pressure drop of 6312 Pa)

Figure 31 shows the SEM of Donaldson (Ultrasonicated Clean) samples. Donaldson media is a thinner dense media which uses surface filtration mechanism. The composition of

Donaldson filter media was not available. It can be seen from the SEM images that the Donaldson media could be synthesized using electro-spun technology. Electro-spun technology is mostly used for polymeric materials. The pore structure is uniform, as seen in Figure 31a. However, the pores between fibers look much smaller compared to our nano-floc embedded filter media. Fibers of different diameters can be seen in Figure 31b. At least two diameter fibers with ca. 2.5 μm and ca. 10 μm can be seen. There is a possibility of some polymer binders included in this media for enhancing the tensile strength. Figure 31c shows the SEM of media after loading salt particulates. The magnified image Figure 31d shows that most of the salt is trapped in the interstitial space between fibers. Some of the salt can be seen attached to the fiber, but not as much compared to the AU Toyobo 2500 Fiber Nano-floc filter media synthesized in our lab.

2.6 Conclusion

The inclusion of nano-fiber flocs composed of Vapor Grown Carbon Fiber (VGCFs) into a fibrous matrix composed of activated carbon fibers and bi-component polymer fibers was studied. Filtration metrics such as filtration efficiency, pressure drop and quality factors were determined for the novel AU nano-floc filter media and was compared against the commercial GOTs media. Due to the slip flow caused by VGCF flocs, the AU nano-floc media was able to capture salt particulates more easily. Additionally, VGCF flocs do not span the entire flow stream contributing to lower resistance i.e. Pressure drop for the flow. Due to the ease of capturing particulate and lower pressure drop, these AU nano-floc fibers showed better filtration performance than the GOTs media. The pressure drop across the media for AU Kynol 1000 Felt, AU Kynol 1000 Cloth Nano-floc filters were lower than the Donaldson (Ultrasonicated Clean) samples, which means that these nano-floc samples consume less power to blow air through the media than the Donaldson sample. The surface filtration mechanism and inclusion of non-porous

media with non-homogeneous pore structures causes higher pressure drops across Donaldson sample. AU Toyobo 1600 Felt and AU Toyobo 2500 Fiber had similar pressure drop as the Donaldson (Ultrasonicated Clean) samples. The Quality Factor metric, which accounts for pressure drop penalty associated with increased filtration efficiency, was better for AU Toyobo 2500 Fiber Nano-Floc filter compared to the Donaldson (Ultrasonicated sample) at different salt particulate loading levels. These results validate that nano-fiber inclusion has a pronounced effect on sea salt aerosol filtration. Additionally, the AU nano-floc media can be easily manufactured using traditional paper making wet-lay technique, which makes it even more attractive for salt aerosol filtration.

Chapter 3: Porosity of Activated Carbon Fibers and its Potential Application on Sea Salt Aerosol Filtration

3.1 Introduction

In the past, carbon felts have been proven to be an excellent sorbent for heavy oil extraction.[19] The sorption capacity of carbon materials was found to be dependent on its bulk density and pore volume.[21] The result from past studies on carbon sorbents suggested that heavy oil can be sucked by capillary forces termed as wicking.[20] Wide variety of fibrous carbon materials are available including fabrics, non-woven felts, activated carbon fibers etc. with high concentration of micropores. Among these, activated carbon is hydrophilic, hence the wicking action can be used to entrap salt aerosol for potential use in sea salt aerosol filtration. This chapter discusses the porous nature of activated carbon fibers and its ability to wick salt aerosol into its pores.

3.1.1 Adsorption of Water on Activated Carbon Fiber

Past study has shown that the water adsorption on pores of activated carbon fibers are due to physical adsorption phenomena and chemical interaction with surface functional groups.[21] The physical adsorption is governed by the Lennard-Jones physical interaction existing between micro-graphitic walls of pores and water molecule, and chemical interaction is governed by the oxygen and other functional groups. Additionally, this study also showed that water adsorption in the pores is influenced by micropore size distribution, with narrower micropores being filled first. Iiyama et al have demonstrated that the water molecular inside the micropore has a solid like structure using electron radial distribution function (ERDF) analysis.[23-25] The adsorption isotherm for activated carbon are S-shaped, have a hysteresis loop and are characterized as Type V in the IUPAC classification, as shown in Figure 32.[26]

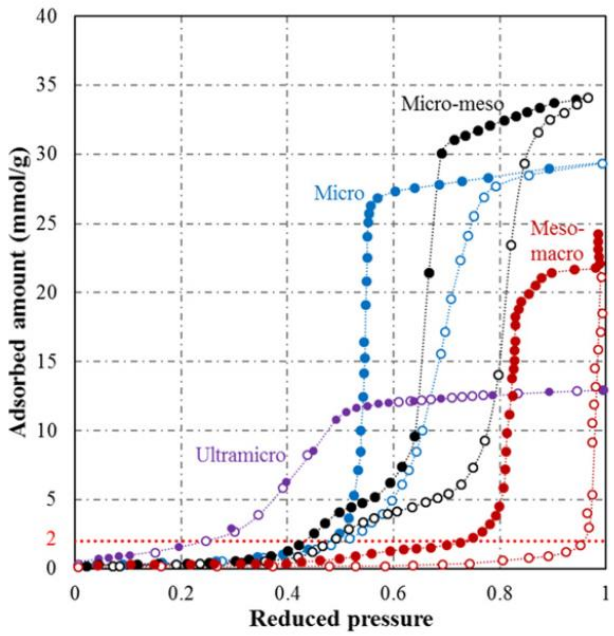

Figure 32. Isotherms for adsorption of water on activated carbon of different porosity[26]

The oxygen functional groups enhance the uptake of water even at low pressures. This is due to the electrostatic partial charges of oxygen functional group. Among oxygen functional groups, carboxylic group showed the highest affinity towards water molecules.[30] It was found that water molecules initially adsorb around the oxygen functional group and then form clusters which grow as more water molecules are added at higher pressure. Nitrogen and sulfur functional groups also have been found to have similar effect on water adsorption.[27-28]

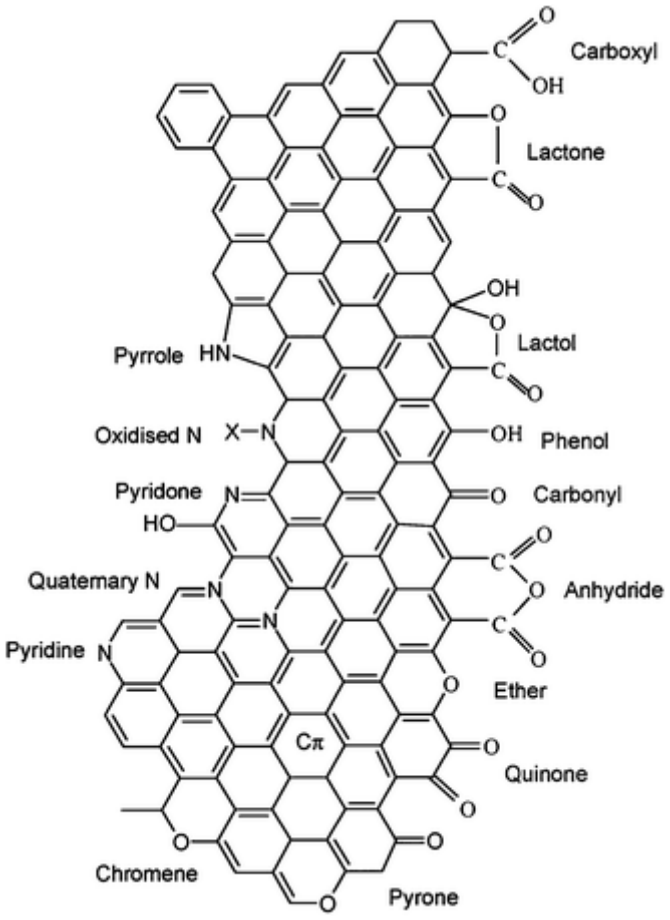

Figure 33. Nitrogen and oxygen surface groups on carbon[29]

However, absorption of water can also be affected by the concentration, location and distribution of functional group, pore size distribution, pore connectivity, temperature etc. Many simulations have been performed in the past to study the effect of these factors on water adsorption on carbon. Figure 34 demonstrates the isotherms for activated carbon fibers of different pore sizes. As the pore size decreases, the hysteresis loop shrinks and disappears for pore size smaller than 0.5nm.[26,31] The adsorption curve shifted to lower reduced pressure with decrease in pore width, so did the desorption curve.

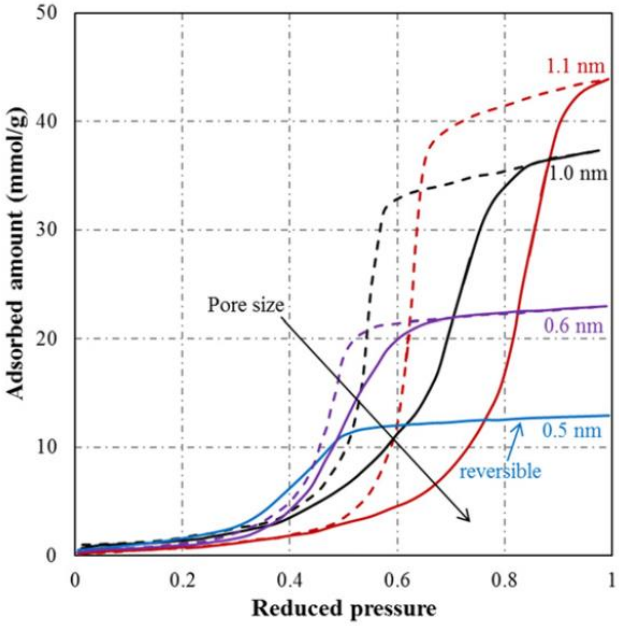

Figure 34. Water isotherm in ACFs with different pore sizes. Solid lines indicating adsorption and dashed line indicating desorption[26,31]

The effect of temperature on water adsorption on activated carbon has been established. Typically, width of the loop decreased with increasing temperature. The evolution of hysteresis loop showed different trends for different temperature ranges.[26]

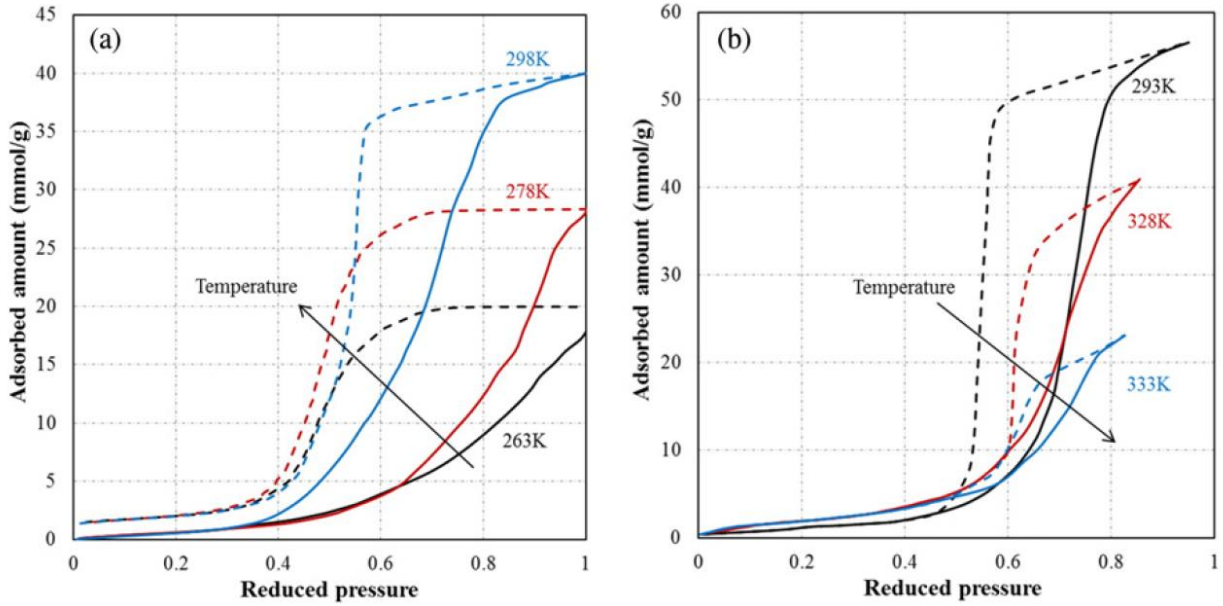

Figure 35. a) Water isotherm for bamboo-based AC at temperature range 263K – 298K[26,32] b) Water isotherm for pitch-based ACFs at temperature range 293K – 333K[26,33]

For the bamboo-based ACF, as the temperature increased, the adsorption curve shifted to lower reduced pressure, but the desorption curve did not shift. This was attributed to improved adsorption capacity of water with temperature.[26,32] For the pitch-based ACFs, the desorption curve shifted to higher reduced pressure with increase in temperature, however the adsorption curve decreases slightly.[26,33] The decrease in adsorption was attributed to decrease in the stability of water clusters with temperature.[34] Based on these results, it was concluded that there exist a threshold temperature of 298K above which water adsorption weakens as the temperature increases, and below which water adsorption increases as the temperature increases.[26]

The water absorption process in carbon is explained in four stages. First the cluster of water forms, secondly the cluster grows and coalesces, thirdly the micropores filling occurs and finally the mesopores fill up.[26] A generalized isotherm is shown in Figure 36. A schematic description of water adsorption in carbon materials is shown in Figure 37.

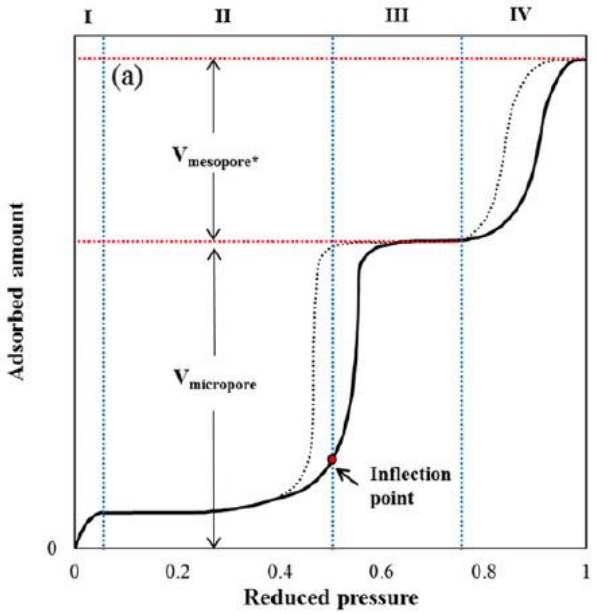

Figure 36. A generalized water isotherm in carbonaceous material explained in four stages I-IV.[26]

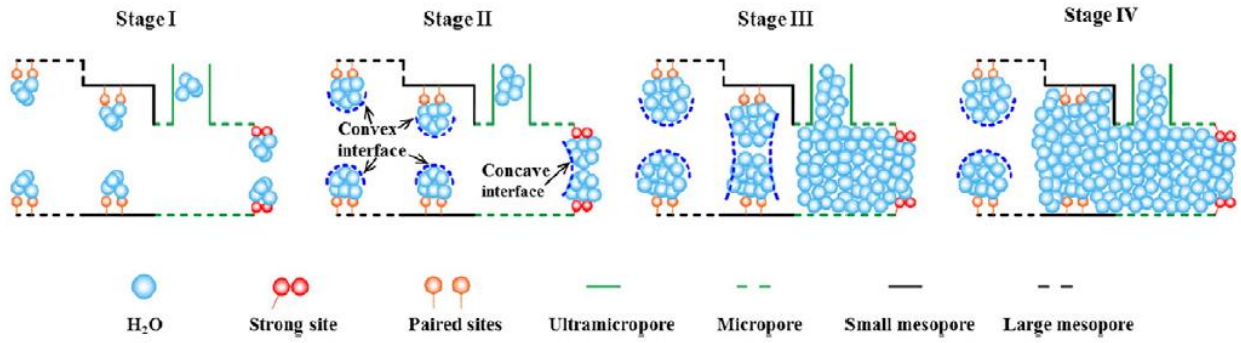

Figure 37. A schematic of water adsorption on carbonaceous material in four stages I-IV[26]

3.1.2 Absorption of Salt Aerosol on Activated Carbon Fiber

Salt aerosol is composed of salt and water. Hence in addition to adsorption process described before, capillary actions also take place during salt aerosol wicking into the pores of activated carbon fibers. The concept of wicking of salt aerosol into the micropores of activated carbon fiber can be explained by Osmotic Pressure, Contact Angle, Young's Equation, Kelvin Equation and Capillary Condensation.

3.1.2.1 Osmotic Pressure

Activated carbon fiber can be visualized as a permeable membrane that allows salt water aerosol on the outside of the fiber to get inside the pores of the fiber. There is an osmotic pressure between the outside and inside. The salt concentration inside the pore is higher than that of the outside. Hence, the salt particulates continuously go inside the pores where there is higher concentration of salt. Therefore, the driving force for this continual salt concentration in pore is the difference in osmotic pressure between the outside salt aerosol and inside salt water. The osmotic pressure of the salt water inside the pore where the concentration of salt is high, is expressed as Equation 8.

$$\pi_H = P_H = \frac{RT}{\bar{V}_W}(X_S)_H \qquad Equation\ 8$$

where π_H is osmotic pressure of salt solution inside the pore, R is ideal gas constant, T is temperature, $(X_S)_H$ is molar fraction of salt inside the pores, $\bar{V}_W$ is partial molar volume of water. When the partial molar volume of water and salt are same, Van't Hoff equation can be obtained.

$$\pi = iCRT \qquad Equation\ 9$$

where i is the Van't Hoff coefficient, C is the salt concentration, R is the gas constant and T is the temperature.[38]

3.1.2.2 Contact Angle and Young's Equation

When liquid wets solid surface, there is a contact angle. Generally, contact angles are measured at equilibrium. There are three different interfaces when liquid wets the solid surface a) solid-liquid interface b) solid-vapor interphase and c) liquid-vapor interphase. The interfacial tension at equilibrium is represented as γ at point where three interfaces intersect, as shown in Figure 38. Young's equation describes this adsorption of liquid droplet on sold surface and is given by Equation 10.[36]

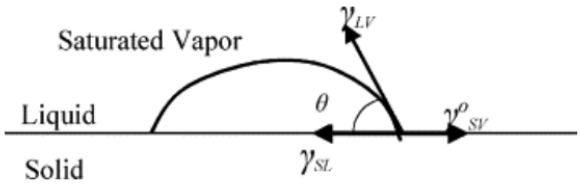

Figure 38: Equilibrium contact angle on a solid surface[36]

$$\gamma_{LV}\cos\theta = \gamma_{SV}^{\circ} - \gamma_{SL} \qquad Equation\ 10$$

$\gamma_{SV}^{\circ} - \gamma_{SL}$ is also called adhesion.

3.1.2.3 Capillary Condensation and Kelvin Equation

At higher RH, activated carbon fibers can adsorb salt aerosol, due to surface tension of salt water in salt aerosol. The salt water in aerosol has low vapor pressure, which allows condensation to occur at the activated carbon fiber pores. The radius of the pores in which salt aerosol will condense can be calculated by Kelvin equation. Kelvin equation demonstrates the effect of curvature of the activated carbon fibers on the free energy of salt aerosol

$$r = \frac{2\gamma V}{RTln(\frac{P}{P_0})} \qquad Equation\ 11$$

where r is Kelvin radius, γ is surface tension of salt water, V is molar mass of salt water, R is gas constant, T is temperature and P/P_0 is relative pressure of salt water. The denominator of Kelvin equation is the free energy of salt aerosol.[37]

3.1.3 Particle Loading Capacity

Particle loading capacity is defined as the quantity of contaminant trapped and held by the filter media before reaching the maximum allowable back pressure drop. Commercial GOTs filter media are thin and dense, and the particle loading curve consists of pressure drop as a function of area density i.e. weight of the total mass of particulate deposited per area of the filter media. The AU nano-floc filter media is a much thicker and porous media. Hence, to fairly compare the thinner GOTs media to AU media, particle loading curve consisting of pressure drop as a function of volume density i.e. weight of the total mass of particulate deposited per volume of the filter media was constructed.

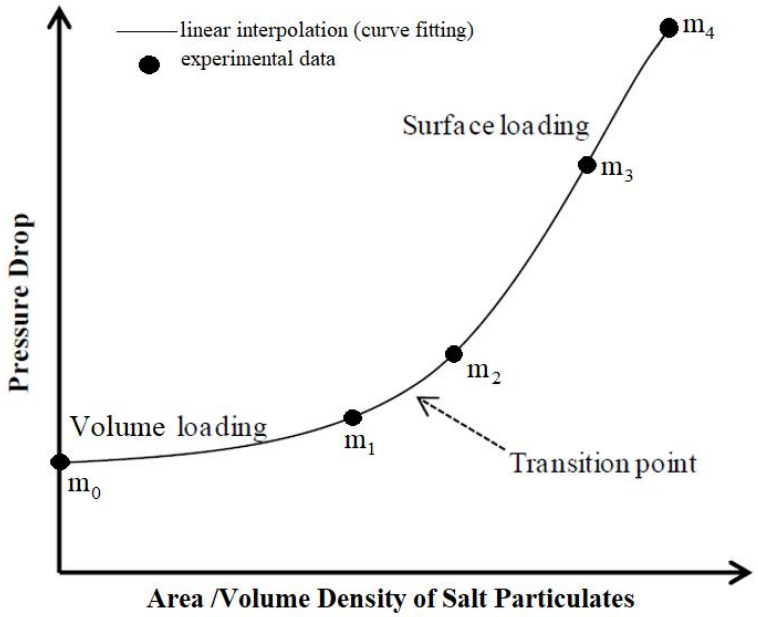

Figure 39. Typical particle loading curve showing different filtration zones

The loading curve is determined by measuring the mass at five instances during the loading process, as shown in Figure 39. The original loading m_0 was recorded, m_1 was recorded near the end of volume filtration zone, m_2 was recorded at the start of surface filtration zone, m_3 was recorded at the middle of surface filtration zone and the final loading m_4 was recorded at the end. It was assumed that the rate of increase in mass loading from one point to other was linear.

3.1.4 Polytetrafluoroethylene (PTFE)

The filter media should have the ability to be regenerated. Not only regenerability increases the lifetime of the filter, it also reduces replacement costs for new filters. Fibrous filters can be regenerated by back-flushing with water, however the back-flush could shed the nano-fibers and cause degradation on filter. A way to prevent the deterioration of the filter during backflush is by applying hydrophobic PTFE coating. PTFE changes the surface chemistry by imparting hydrophobicity, consequently preventing the water to shed the fibers during backflush. PTFE also has low surface energy further preventing surface to be wetted by water. PTFE available in liquid

emulsion was diluted and sprayed over the surface of the filter. In addition to enhancing surface integrity, it also has the potential to prevent aqueous flooding, enhance filtration and resist clogging. PTFE imparts hydrophobicity which changes the surface chemistry including wettability, contact angle. For a silk coated with PTFE, the contact angle increased from 68 to 138.[39] In addition, PTFE has great thermal stability up to 240°C, which means it can be dried easily after backflush. PTFE has been traditionally used in industry to make stain repellant and thermal-resistant clothing.[40] Hence performance of PTFE coated filters along with other filter media were studied and the results are discussed in subsequent sections.

3.1.5 Hypothesis

Based on the scientific background discussed in the previous sections, it was hypothesized that the salt particulates continuously load into the wet activated carbon pores, and this process pauses only after water dries out and salt saturates in the pores. Depending on the RH (i.e the partial pressure), above the carbon fiber, salt either goes inside the pores or remains outside. Lowering the RH promotes slow drying and the concentration of the salt in the droplet increases. Salt goes to water because solubilizing helps reduce surface energy. Water dries out of macropores faster, after that the salt gets pulled into the micropores. As long as the micropores remain wet, continuous loading of the salt into wet micropores take place until it reaches saturation. Hence water in the wet pores is the driving force for continuous salt entrapment until saturation. Another hypothesis made was that the hydrophobic PTFE layer coated on the AU Toyobo 1600 Felt Nano-floc filter media will prevent water to flood the depth of the filter media. This could potentially only allow salt to penetrate the depth of the filter, further enhancing the particle loading capacity of the filter. This could also potentially help with regeneration of the media during backflush

operation. Experiments were performed and the results discussed in subsequent chapters to test these hypotheses.

3.2 Experimental

3.2.1 Salt Absorbed by AU Toyobo 1600 Felt Nano-floc Filter Media

AU Toyobo 1600 Felt Nano-floc filter media was soaked in 2.5 wt% salt water overnight. The media was dried at 140F overnight and the sample was weighed. The difference in mass gave the amount of salt absorbed by the filter media per volume.

3.2.2 Pore Volume and Surface Area Calculations

For different types of activated carbon fibers used to prepare the nano-floc embedded filter media, the pore volume and potential mass of activated carbon entrapped into the pores at saturation was calculated.

3.2.3 Droplet Formation on the PTFE Coated AU Toyobo 1600 Felt Nano-floc Filter Media

A dropper was used to dispense a droplet of water on the AU Toyobo 1600 Felt Nano-floc filter media, to see the effect of PTFE on the absorption of water into the depth of the filter media. Microscope by Nikon was used to track the changes in the droplet structure for both PTFE coated and non-coated AU Toyobo 1600 Felt Nano-floc filter media. The micrographs are included in next section.

3.2.4 Salt Aerosol Concentration

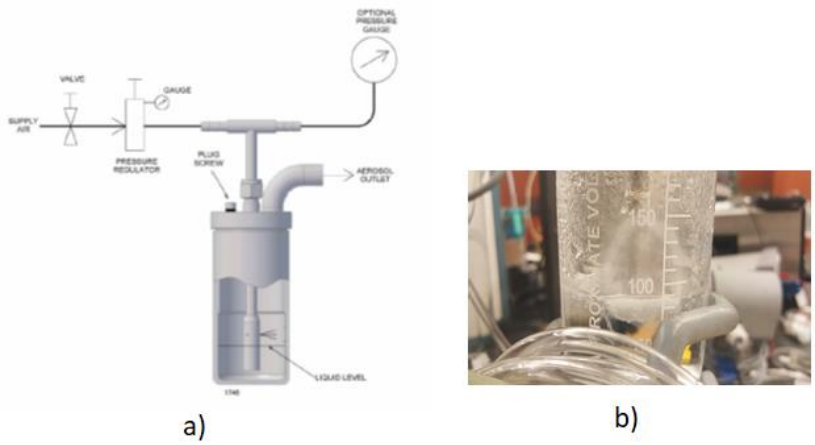

a) b)

Figure 40. a) A collision nebulizer schematic b) Collision nebulizer generating salt aerosol

A 2.5% w/w NaCl solution was applied in a Collision nebulizer to generate salt aerosol needed for the experiments as shown in Figure 40. A method was developed to estimate the salt concentration in the upstream. The concentration of salt in the aerosol flowing in the air stream is measured in parts per million by weight (ppmw), and is defined by equation 12, where c_{salt} is the concentration of salt in ppmw, m_{salt} is the mass of sea salt (g) and m_{air} is the mass of air (g).

$$c_{salt} = \frac{m_{salt}}{m_{air}} * 10^6 \quad Equation\ 12$$

An assumption was made that all salt particulates are captured after filter media clog, causing the pressure drop across the media to increase exponentially. The difference of mass between fully loaded sample and the clean sample gives the mass of salt particulates gathered from the aerosol upstream. GOTs media was applied for this purpose to capture salt particles.

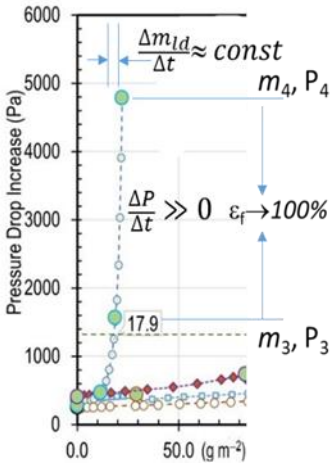

Figure 41. Assessment of salt content in upstream aerosol by assuming that all salt aerosols are captured by the clogged filter media

The change in mass for the GOTs media is $m_{salt} = 1.70 \times 10^{-3}$ g, when pressure rapidly increases from t_1 to t_2 (Figure 41, $\Delta t = t_2 - t_1$). The total volume of air passing through the media during this period is 132 liters at 21.7 cm/s within 20 minutes. Thus, concentration of salt in the aerosol upstream was calculated as 9.95 ppmw.

$$c_{salt} \approx \frac{1.7 * 10^{-3}}{(132/22.4) * 29} (* 10^6) = 9.95 \text{ ppmw}$$

3.2.5 Particle Size Distribution of Salt Aerosol

In order to load the salt aerosol into the filter media for determination of particle loading curves, one-jet Collison nebulizer is suitable, since it generates higher concentration salt aerosol with consistency. However, there is an upper limit to the amount of salt aerosol that the LAS-XII particle counter can handle. Since Hudson micro-mist nebulizer has lower consistency and reliability, it cannot be used for accurate particle size distribution. Hence Collision nebulizer with dilution mechanism is applied for salt aerosol particle size distribution. The concentrated aerosol stream generated by the Collision nebulizer was diluted in dry air twice to obtain a face velocity of 21.7 cm/s. The sampling portion of the aerosol was calculated as 0.00826%.

The LAS-XII particle counter can detect particle ranging from 0.09 to 7.5 µm. The salt aerosol generated by nebulizer generally have lognormal size distribution, which is the best for single source aerosols.[41] The Collision nebulizer generates polydispersed salt particles with a wider size distribution. The width of the laser bins affects proper determination of aerosol concentration. The resolution problem can be avoided by using normalized concentration ($dC_{n,i}/dlogD_{p,i}$). The $dlogD_{p,i}$ element is adopted to normalize the bin width through width subtraction of upper bin boundary from the lower bin boundary. This gives a normalized concentration value that is independent of the bin width.[42] The salt aerosol particle size distribution for Collision nebulizer was obtained as shown in Figure 42. The particle size ranges from 95 nm to 1000 nm, with majority of the particles ranging in diameter from 95 nm to 500nm. The salt aerosol of 9.95 ppmw are normally applied to load the filter media at 21.7 cm/s face velocity for particle loading experiments.

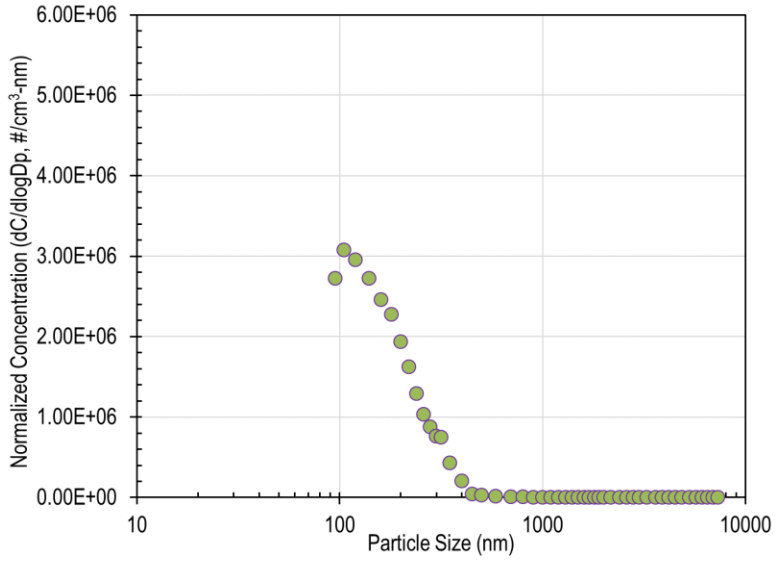

Figure 42. Normalized salt aerosol concentration vs particle diameter for aerosol generated by Collision nebulizer (at outlet) using 2.5% NaCl salt solution and 1.2 slpm air flow

3.2.6 Particle Loading Capacity

For different media used, the particle loading curves were obtained and the results were compared at the breakthrough pressure drop values. The AU Toyobo 2500 Fiber Nano-floc media were compared against Donaldson (Ultrasonicated Clean) samples. The particle loading was determined by taking the sample out of the filtration setup and drying it. Also, AU Toyobo 2500 Fiber Nano-floc media coated with 6% PTFE solution (made from 60% PTFE solution) with various amounts of PTFE coating was also included in the study. The particle loading curve was constructed by measuring the mass multiple times during the particle loading process, and the rest of the curve was fitted by assuming a linear mass loading increase between two consecutive experimentally measured points.

3.2.7 Regeneration of AU Toyobo 2500 Fiber Nano-floc Filter Media

Regeneration of filter media offers many advantages. Not only does it help to extend the life of the filter, but also reduces the need for replacing new filters consequently lowering maintenance and operation cost. To study the regenerability of nano-floc media developed in our lab, AU Toyobo 2500 Fiber Nano-floc Filter Media without PTFE coating and with 1.28g/m^2 PTFE coating were compared against the industrial GOTS sample. The regenerated media's performance was measured by plotting particle loading curves, and Quality Factor plots. For regeneration all the samples were sonicated in water for 30 minutes. The salt particles dissolved in water, and the salt particulates visible on the surface before were not visible after regeneration. The samples were dried in oven at 140 °F overnight. 2.5% w/w NaCl solution were used in one-jet collision nebulizer to generate 9.95 ppmw salt aerosol. 1.2 slmp of air was blown into the nebulizer, while 1.9 slpm of dry air was supplied to a glass bubbler with water to generate relative humidity of 72%.

3.3 Results and Discussion

3.3.1 Pore Volume and Surface Area Calculations

Activated carbon fiber can be commercially found in many forms including fibers, clothes, felt etc. These activated carbons can have different surface area. Depending on the salt water absorbed, the pore volume of these activated carbon per gram of samples were calculated. Additionally, pore volume per area of sample and potential mass of salt entrapped per area of sample was also calculated. The results are tabulated in Table 2.

No.	**ACF Type**	**BET Surface Area (m^2/g)**	**Pore Volume per g of sample (cm^3/g)**	**Pore Volume per cm^2 of sample (cm^3/cm^2)**	**Potential mass of NaCl dissolved in ACF (g/m^2)**
1.	Kynol Cloth	1000	0.468	0.008	26
2.	Kynol Felt	1000	0.582	0.01	32
3.	Toyobo Felt	1600	0.797	0.014	45
4.	Toyobo Fiber	2500	0.88	0.015	48
5.	Glass Fiber	N/A	0	0	0

Table 2. Pore volume and potential mass of salt entrapped by activated carbon fibers

The results demonstrated that Toyobo Fiber with 2500 m2/g BET surface area has the highest pore volume and consequently highest potential mass of NaCl entrapped i.e. 48 g/m2. It can also be observed that larger the pore volume, higher the potential mass of NaCl entrapped.

3.3.2 Droplet Formation on the PTFE Coated AU Toyobo 1600 Felt Nano-floc Filter Media

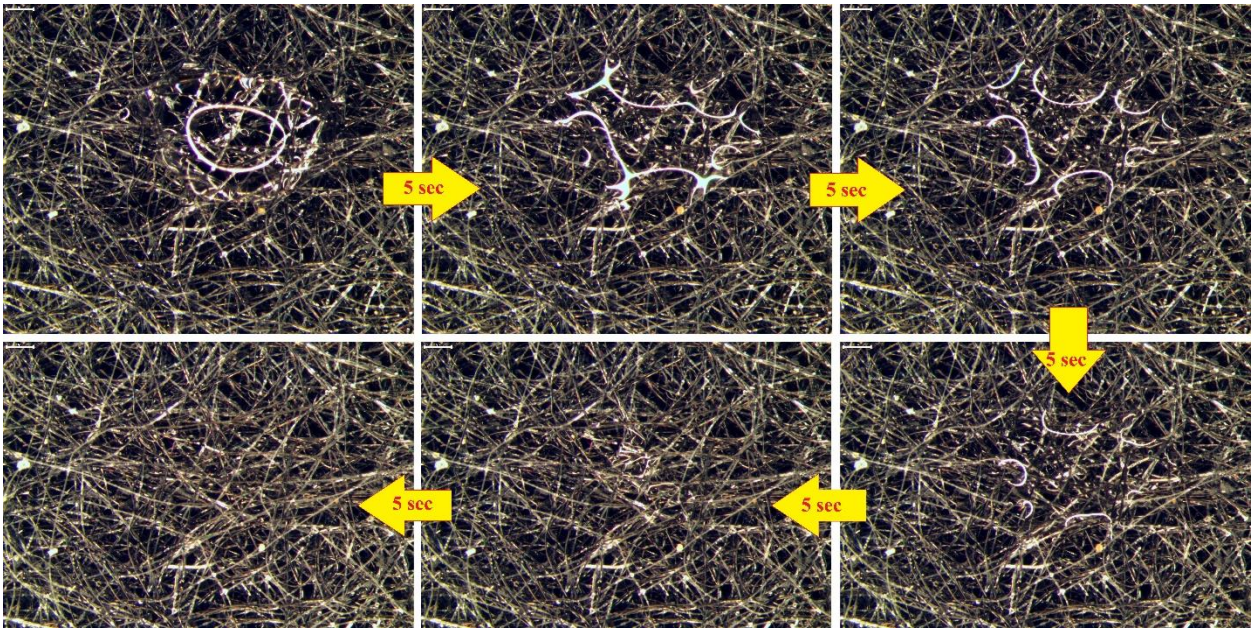

Figure 43. Micrograph of water absorption by AU Toyobo 1600 Felt Nano-floc filter media in 5 second increments. The scale on top left corner of each micrograph is 1 micron in length.

It can be seen from Figure 43 that for AU Toyobo 1600 Felt Nano-floc filter media without any PTFE absorbs a droplet of water completely into its pores within 25 seconds. This image further verifies that the porous nature of activated carbon fiber and its hydrophilicity is very effective in entrapping water or sea aerosol into its pore. The circular ring on the water droplet seen on the top left image is the reflection of light from microscope lamp on the droplet.

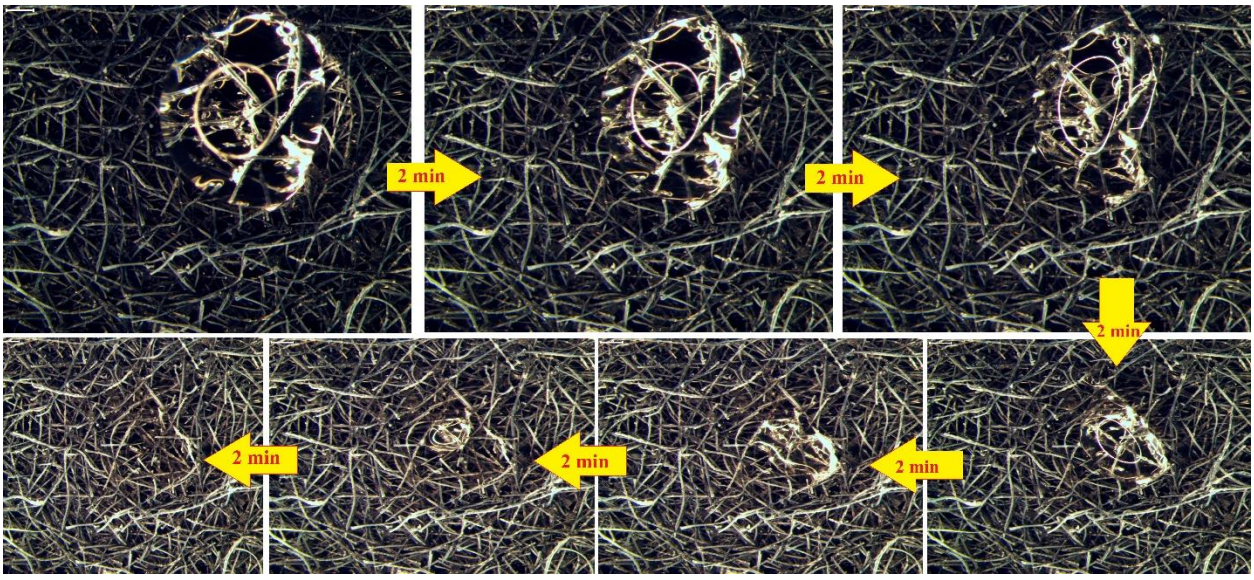

Figure 44. Micrograph of water absorption by AU Toyobo 1600 Felt Nano-floc filter media coated with 3.22 g/m^2 PTFE in 2-minute increments. The scale on top left corner of each micrograph is 1 micron in length.

Figure 44 shows the AU Toyobo 1600 Felt Nano-floc filter media coated with 3.22 g/m^2 PTFE. Since PTFE is hydrophobic, the fluorine functional groups of PTFE will help keep the water off the filter media, and potentially avoid aqueous flooding. The surface fibers are coated with PTFE, but the water droplet eventually disappear after 12 minutes. This is mostly due to evaporation of the droplet of water. However, some of the water is still absorbed by small percentage of activated carbon fibers on the surface that did not get the PTFE coating. This can be fixed by increasing the amount of PTFE. However, too much PTFE also increases pressure drop due to PTFE layer formation on surface fiber. Hence an optimal PTFE loading needs to be determined for better filtration performance.

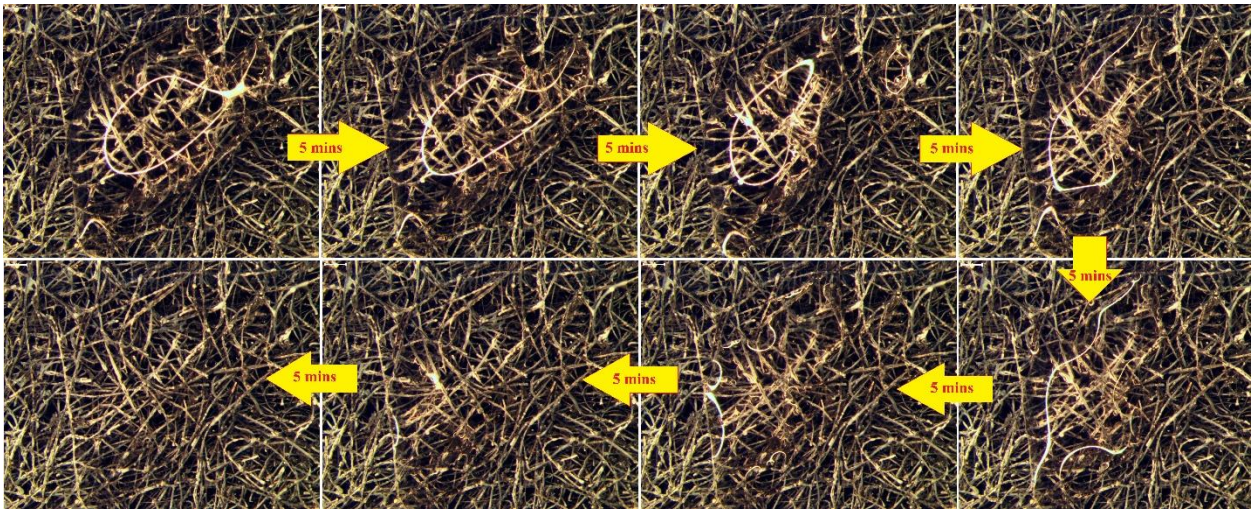

Figure 45. Micrograph of water absorption by AU Toyobo 1600 Felt Nano-floc filter media coated with 9.02 g/m^2 PTFE in 5-minute increments. The scale on top left corner of each micrograph is 1 micron in length.

As discussed previously, coating more PTFE seem to increase the time required to evaporate the water droplet, as seen in Figure 45. Coating 9.02 g/m^2 PTFE, the water droplet disappeared after 35 minutes. Increasing PTFE coating further increases the time to evaporate the droplet. However, too much PTFE coating can significantly increase pressure drop across the filter media. Therefore, and optimal PTFE coating should exist where the filtration efficiency is high, but the pressure drop is not unacceptable.

3.3.3 Particle Loading Capacity

Higher quality filters can withhold high levels of particulates before reaching an unacceptable levels of pressure drop. Particle loading capacity is another critical parameter that helps to assess filter media performance, besides filtration efficiency and pressure drop. The particle loading capacity is defined as the quantity of contaminant trapped and held by the filter media before reaching the maximum allowable pressure drop. The particle holding capacity of a filter media is strongly associated with its lifetime and is an important design parameter. Higher

particle loading capacity can help avoid replacement costs of filters. AU Toyobo 2500 Fiber Nano-floc filters samples along with Donaldson samples were tested under different RH condition. Since salt aerosol act different at low RH and at high RH, three RH levels 1) 8-10% 2) 50% and 3) 72% were tested.

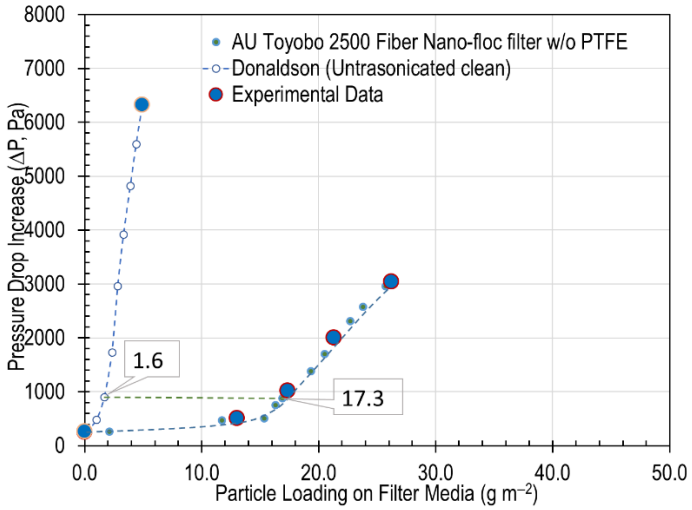

Figure 46. Particle loading capacity at 8-10% RH

Particle loading curve of AU Toyobo 2500 Fiber Nano-floc filter media and Donaldson (Ultrasonicated Clean) media at low RH i.e. 8-10% was generated by plotting pressure drop across the media as a function of salt particle loading in g/m^2. The values at the breakthrough point are labelled in the graph. It can be seen from Figure 46 that the particle loading in g/m2 of the AU Toyobo 2500 Fiber Nano-floc filter media is 10.8 times larger than that of the commercial Donaldson filter media sample. The porous nature of the activated carbon fibers can accommodate more salt particulates into its pore by capillary action, hence the particle loading is significantly higher for AU nano-floc media. Donaldson filter is most likely made of non-porous polymer fibers via electro-spun or melt-blown technology, hence it cannot absorb salt aerosol. Therefore, it has very low particle loading capacity. In addition, the Donaldson media is a dense and thin media which uses surface filtration mechanism, while the AU nano-floc media is highly porous and much

thicker media which uses volume filtration mechanism. The volume filtration mechanism allows particles to be entrapped into the interstitial spaces between fibers too.

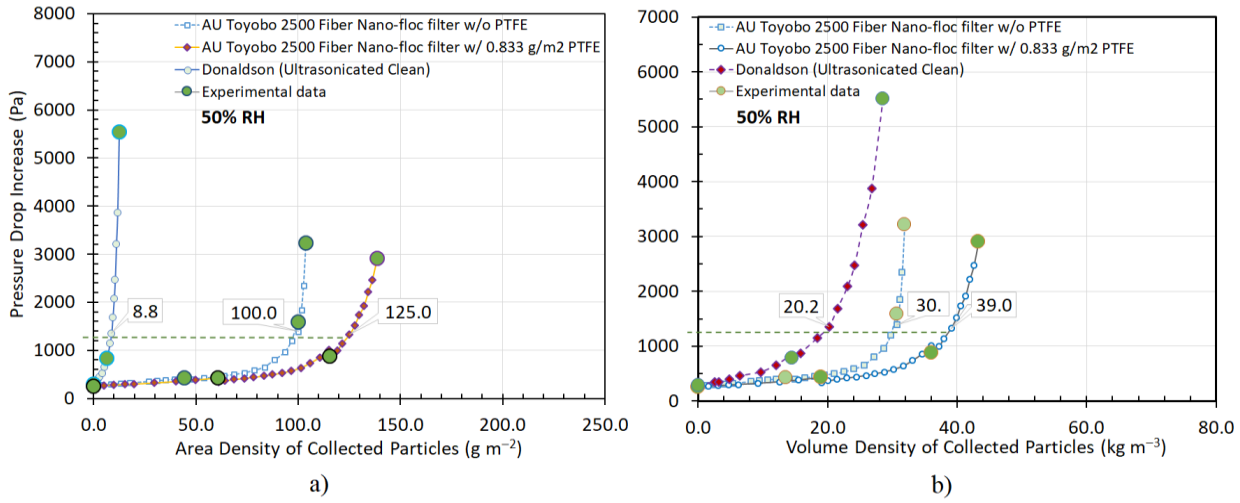

Figure 47. Particle loading capacity in terms of a) Area Density and b) Volume Density for different filter media at 50% RH

The particle loading capacity of AU Toyobo 2500 Nano-floc filter without PTFE and with 0.83 g/m^2 PTFE, along with industrial Donaldson (Ultrasonicated clean) sample at 50% RH was generated by plotting area density and volume density against pressure drop. The volume density gives a more accurate picture of particle loading capacity because it accounts the thickness of the media as well, since the Donaldson is much thinner compared to AU nano-floc media. The breakthrough pressure drop point was determined and is labeled in the plot. The area density is just grams of salt deposited on the filter media per m^2 of the filter media, while the volume density is the kilograms of salt deposited on the filter media per m^3 of the filter media. The volume density was obtained by multiplying the area density by the thickness of the media. It can be seen from Figure 47 that the area density of the AU Toyobo Nano-floc filter with 0.833 g/m^2 PTFE has 125 g/m^2 of salt at the breakthrough point, which is 1.25 times larger than that of AU Toyobo Nano-floc filter without PTFE and 14.2 times larger than that of industrial Donaldson sample. Similarly,

the volume density of AU Toyobo Nano-floc filter with 0.833 g/m^2 PTFE has 39 kg/m^3 of salt at the breakthrough point, which is 1.3 times larger than that of AU Toyobo Nano-floc filter without PTFE and 1.9 times larger than that of industrial Donaldson sample. From above discussion, it can be concluded that the AU Nano-floc filter has much better salt loading capacity than the industrial sample. Also, optimal PTFE coating of 0.833 g/m^2 further improved the particle loading capacity.

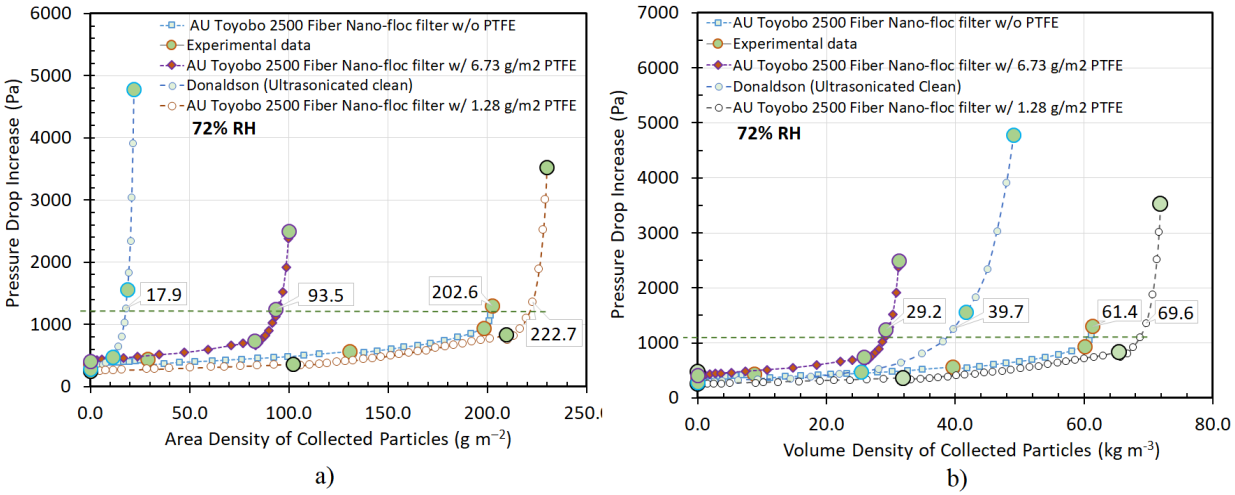

Figure 48. Particle loading capacity in terms of a) Area Density and b) Volume Density for different filter media at 72% RH

Particle loading experiments were performed at 72% RH for AU Toyobo 2500 Fiber Nano-floc Filter Media without PTFE, with 1.28 g/m^2 PTFE, with 6.73 g/m^2 PTFE, along with industrial Donaldson (Ultrasonicated Clean) sample. Particle loading values at breakthrough points were recorded and can be seen in Figure 48. The AU Toyobo 2500 Fiber Nano-floc Filter Media with 1.28 g/m^2 PTFE showed the highest area density value of 222.7 g/m^2 at the breakthrough point, which is 1.1 times that of the AU Toyobo 2500 Fiber Nano-floc Filter Media without PTFE, and 12.4 times that of the Donaldson (Ultrasonicated Clean) sample. Interesting observation was made for AU Toyobo 2500 Fiber Nano-floc Filter Media with 6.73 g/m^2 PTFE. The area density after increasing PTFE loading from 1.28 to 6.73 g/m^2 decreased from 222.7 g/m^2

to 93.5 g/m^2. This is due to more PTFE creating a layer on the surface fibers, blocking the particulates to penetrate the depth of the media, resulting in decreased area density. Hence an optimal PTFE coating should be determined so that the PTFE layer does not clog the surface and prevent particle from entering the depth of the media. A more accurate particle loading capacity of filter media is determined in terms of volume density, since it also considers the thickness of the media. This is important when packaging and pleating is considered, when only so much of the media can be fitted per volume. The particle loading capacity, in terms of volume loading for AU Toyobo 2500 Fiber Nano-floc Filter Media with 1.28 g/m^2 PTFE was recorded as 69.6 kg/m^3 at the breakthrough point, which is 1.13 times that of the AU Toyobo 2500 Fiber Nano-floc Filter Media without PTFE and 1.75 times that of the Donaldson (Ultrasonicated Clean). Interestingly, the volume loading of AU Toyobo 2500 Fiber Nano-floc Filter Media with 6.73 g/m^2 PTFE, was 29.2 kg/m^3, which is even lower than that of the Donaldson (Ultrasonicated Clean) sample. Hence this further validates that using too much PTFE is detrimental to the dirt holding capacity of the filter media.

3.3.4 Regeneration of AU Toyobo 2500 Fiber Nano-floc Filter Media

It was hypothesized that PTFE can potentially help with regeneration of the media. AU Toyobo 2500 Fiber Nano-floc filter media with different amount of PTFE coating was regenerated by soaking the media in water, to allow the salt particulates to dissolve back into the water. After dissolving the salt particulates back into the water, the samples were dried in oven and the particle loading experiment was performed for the second cycle. However, the regeneration of Donaldson sample was performed by sonicating the sample in water for 30 minutes. The particle loading curves were plotted and compared against the results from first cycle (i.e. before regeneration).

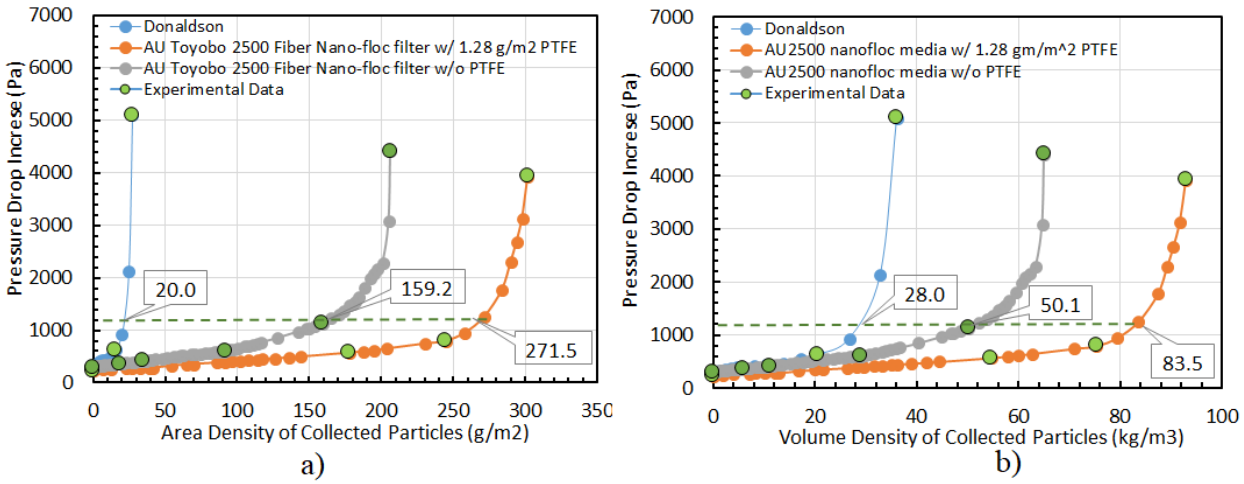

Figure 49. Particle loading capacity in terms of a) Area Density and b) Volume Density for different filter media at 72% RH

Sample	1st cycle of filtration		2nd cycle of filtration (after regeneration)	
	Area density (g/m^2)	Volume density (kg/m^3)	Area density (g/m^2)	Volume density (kg/m^3)
Donaldson	17.9	39.7	20	28
AU Toyobo (w/o PTFE)	202.6	61.4	159.2	50.1
AU Toyobo (w/ 1.28 g/m^2 PTFE)	222.7	69.6	271.5	83.5

Table 3. Comparison of particle loading capacity in terms of a) Area density and b) Volume density before and after regenerating filter media

It can be seen from Table 3, that after regeneration the volume density of Donaldson decreased from 39.7 kg/m3 to 28 kg/m3, whereas that of AU Toyobo 2500 Fiber Nano-floc filter media without PTFE decreased from 61.4 kg/m3 to 50.1 kg/m3. However, the volume density of AU Toyobo 2500 Fiber Nano-floc filter media with 1.28 g/m2 PTFE increased significantly from 69.6kg/m3 to 83.5 kg/m3. Hence this validates that PTFE affects filtration media drastically by increasing the particle holding capacity.

Although particle loading capacity increases after regeneration as discussed before, the filtration efficiency might not be better, or the pressure drop penalty might be too high resulting in lower quality factor. Hence it is vital to study the effect of PTFE on filtration efficiency and quality factor. Figure 50 shows the filtration efficiency before and after regeneration for AU Toyobo 2500 Fiber Nano-floc filter with and without PTFE, and Donaldson samples. It can be seen from Figure 50a that the filtration efficiency doesn't change for Donaldson media. However, the filtration efficiency of the AU Toyobo 2500 Fiber Nano-floc filter w/1.28 g/m^2 PTFE for particle range 95-300 nm increases further after regeneration. Also, the AU Toyobo 2500 Fiber Nano-floc filter w/o PTFE for particle range 95-180 nm increases further after regeneration. This shows that the nano-floc filter media can endure regeneration process without affecting filtration efficiency. Also, the quality factor of Donaldson does not change after regeneration. However, for AU Toyobo 2500 Fiber Nano-floc filter w/1.28 g/m^2 PTFE, the Quality Factor increases across entire particle size range. The AU Toyobo 2500 Fiber Nano-floc filter w/o PTFE increases for particle diameter range 95 nm to 300 nm but decreases from 300 nm to 100 nm. This further validates that the little amount of PTFE coating can enhance the dirt holding and filtration efficiency without unacceptable increase in pressure drop. There is no penalty such as deterioration of the structure or pressure drop increase associated with the improvement in particle loading capacity with PTFE inclusion.

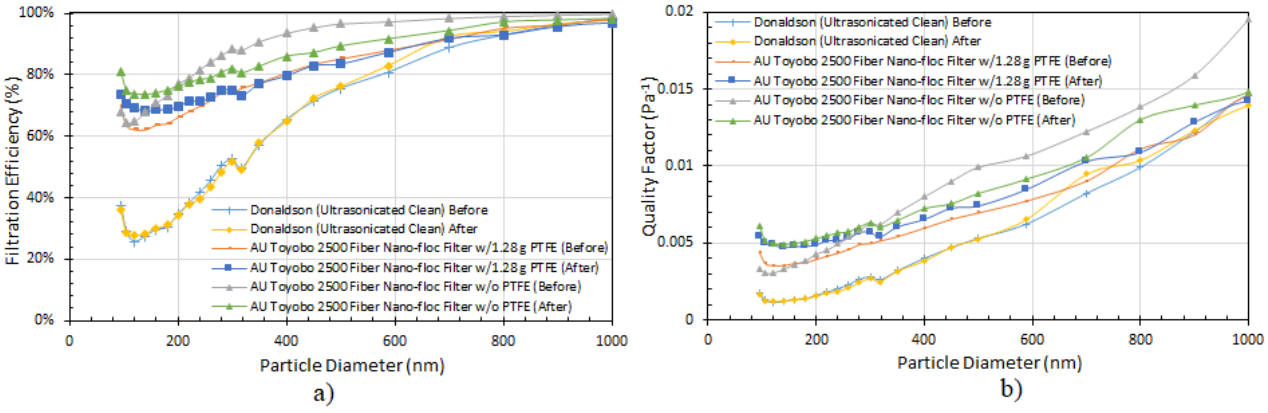

Figure 50. Filtration efficiency and Quality Factor of AU Toyobo 2500 Fiber Nano-floc filter w/ and w/o PTFE and Donaldson (Ultrasonicated Clean) samples before and after regeneration

3.4 Conclusion

The absorption of salt aerosol in the pores of activated carbon can be described by capillary forces, and adsorption isotherms. The osmotic pressure difference between the salt aerosol on the surface of the activated carbon fiber and salt water inside the pores causes more salt to be wicked into its pores, since the salt water inside is more concentrated. Hence, as long as saturation is not achieved, salt keeps getting wicked into the pores of activated carbon fiber. Also due to high surface tension of the water inside the pores and low vapor pressure, it gets condensed inside the pores. Considering this nature of activated carbon fibers, the particle loading capacity of the AU nano-floc media containing ACFs were studied to see if there is any enhancement in particle loading capacity due to this multifaceted phenomenon. The potential mass of salt absorbed by different kinds of activated carbon fibers showed that up to 48 g/m2 of salt can be entrapped inside the pores. At low RH, i.e. 8-10%, the particle loading capacity of AU Toyobo 2500 Fiber Nano-floc filter media was found to be 10.8 times higher than that of the Donaldson (Ultrasonicated Clean) sample. At medium RH, i.e. 50%, the particle loading in terms of volume density for AU Toyobo 2500 Fiber Nano-floc filter media with 0.83 g/m2 PTFE was 1.9 times that of the Donaldson (Ultrasonicated Clean) sample. At high RH, i.e 72%RH, the particle loading in terms of volume density for AU Toyobo 2500 Fiber Nano-floc filter media with 1.28 g/m2 PTFE was 1.75 times higher than that of the Donaldson (Ultrasonicated Clean) media. However, increasing PTFE coating to 6.73 g/m2 significantly decreased the particle loading capacity of AU Toyobo 2500 Fiber Nano-floc filter media, even below Donaldson (Ultrasonicated Clean) sample. It was attributed to excessive PTFE creating a layer on surface, preventing the particulates to

penetrate the media. Hydrophobic PTFE inclusion onto filter media was also performed to study the enhancement in filtration performance and observe its effect on regeneration. The regeneration of AU Toyobo 2500 Fiber Nano-floc filter media with 1.28 g/m2 increased the volume density from 69.6 kg/m3 to 83.5 kg/m3. This validated the effectiveness of PTFE in regeneration of AU nano-floc media. The increase in particle loading did not have any penalty associated with it, as the quality factor remained the same after regeneration.

Chapter 4 Influence of Hydrophobic PTFE Coating on Filtration Efficiency and Quality Factor Metrics

4.1 Introduction

In the previous chapter, it was demonstrated that some amount of PTFE coating on filter media enhances the particle loading capacity of the filter media. It was also found that too much PTFE coating decreased the particle loading capacity of the media. So, it is essential to optimize the amount of PTFE that is to be coated onto the filter media for enhanced performance. Previous chapter also presented work on regeneration of the media, where it was observed that PTFE coating increased the particle loading capacity after regeneration. However, dirt holding capacity is not the only metric used to judge a filter media. The filtration efficiency and quality factor also need to be considered, because the media could have changes in structure after regeneration. In this chapter, the filtration efficiency and Quality Factor of AU Toyobo 1600 Felt Nano-floc filter media was studied by varying the amounts of PTFE coatings and by conducting filtration at different levels of RH. Once the quality factor is achieved, it can be used along with the particle loading curves to select the appropriate media. Some applications that require high quality air want filters with high particle loading capacity but do not care much about the pressure drop penalty. On the other hand, some applications are willing to compromise with the quality of air to some extent but want to minimize energy cost associated with pressure drop. Hence there is a tradeoff between particle loading capacity and quality factor of filter media and both should be considered while designing or selecting a filter media.

The relative humidity (RH) in the ocean environment is significantly higher compared to land. The presence of such high level of RH can affect the performance of filter media including pressure drop, filtration efficiency, quality factor and particle loading capacity. RH is the ratio of

the partial pressure of water vapor in an air-water mixture to the saturated vapor pressure of water at a prescribed temperature.[1] Sodium chloride particles are hydrophilic particles with a deliquescent point of 72% RH. Above it, the sodium chloride particles become saturated as liquid particles (droplets) and below it the sodium chloride particles act as hydrated particles.[1] Hence, two RH values (30% and 50%) below the deliquescent point and one RH value (72%) at the deliquescent point was selected for this study.

The properties of filter media and their interaction with both wet and dry sea salt aerosol is significantly affected by the surface chemistry, contact angle and surface free energy of the media. These interfacial interactions are also important for potential regeneration and back-flush operations. Hence, additive properties of hydrophobic Polytetrafluoroethylene (PTFE) aka Teflon was studied by coating the media with 2.5 wt% solution made from 60 wt% PTFE emulsion, using the Hudson RCI Micro-mist Nebulizer. PTFE provide the functional fluorine group that imparts hydrophobicity onto the surface fibers, potentially keeping the water off the filter media and improving the penetration of salt particulates into the depth of the media. This will enable the utilization of entire volume of the media and prevent aqueous flooding. Enhancement in particle loading capacity with PTFE coating has been demonstrated in previous chapter, however effect of PTFE on filtration efficiency and Quality Factor will be further tested in this chapter.

4.1.1 Filter Media Used

To study the effect of hydrophobic PTFE coating on filtration efficiency and Quality Factor, AU Toyobo 1600 Felt Nano-floc Filter media was used. The AU Toyobo 1600 Felt Nano-floc Filter media was coated with different amount of PTFE solution using a Hudson Micro-mist Nebulizer and filtration were conducted at different RH to study its effect.

4.2 Experimental Methods

4.2.1 Synthesis of AU Toyobo 1600 Felt Nano-floc Filter Media

AU nano-fiber filter is sinter locked network of fibers with nano fiber flocs embedded between bi-component polyester/polyethylene fiber as shown in Figure 17c. Although nanofiber has been used to generate filer media using electro-spun or melt-blow processes, these fibers are two dimensional and lack the strength required for high level salt aerosol loading. Hence VGCF flocs were synthesized and embedded within polyester microfibers to create a three-dimensional media with better strength and particle loading capacity. In addition, this media is scalable to industrial level. Improvement in filtration efficiency after entrapping VGCF flocs were confirmed by Zhao[1]. The filtration efficiency improved up to 99.7% for 1.86% VGCF and it was attributed to smaller pore diameter after entrapping VGCFs. However, pressure drop was significantly higher. An optimal VGCF of 1.31% showed good permeability and Quality Factor higher than the sample without VGCF.[1] This improvement is a combined effect of nano fiber inclusion, change of conventional flow to slip-flow resulting in lower pressure drop, and slip flow causing particle to travel closer to fiber increasing filtration efficiency.

4.2.2 Bench-Scale Filtration Setup

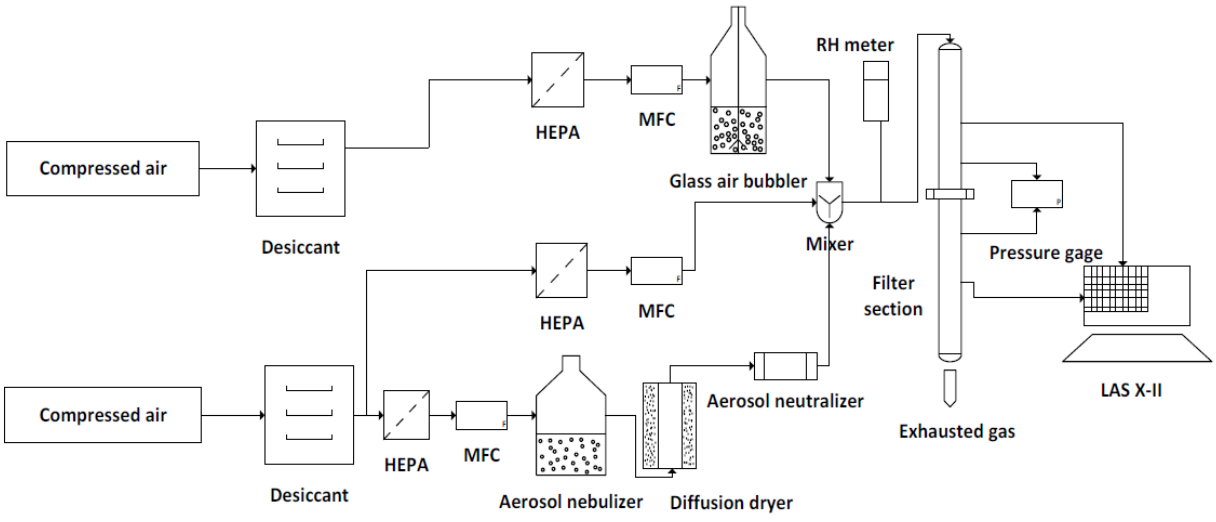

Figure 51. Schematic of experimental setup for filtration test with humidity control

The experimental setup for testing performance of different media for salt aerosol filtration is shown in Figure 51. Compressed air was passed through the desiccant containing silica gels to remove the moisture, followed by High Efficiency Particulate Air (HEPA) filter to get rid of any contaminants. Out of the three streams flowing through the process, the first is the nebulizing air stream. The nebulizing air stream was used to generate aerosol with salt particulates. The flow rate of nebulizing air was controlled using a mass flow controller. Sodium chloride (NaCl) solution (5% [w/w]) was used in all experiments. Hudson RCI micro mist nebulizer from Teleflex Medical was used to generate the salt aerosol. The wet aerosol was dried by passing it through a diffusion dryer (DD 250) manufactured by Air Techniques International. Aerosol neutralizer (Model-9000) by Brechtel and two Polonium-210 strips by NRD, LLC were used to neutralize the static charges developed due to aerosolizing. A second stream of air was mixed with the neutralized salt particle aerosol to dilute it to ensure that the concentration of salt particle does not exceed the limit handled by the LAS-XII particle counter. Third air stream was passed through a glass bubbler with deionized water to generate humidity. A mass flow controller was used to control the flow rate of air passing through the bubbler to control the RH level. Finally, all the streams were combined and passed through the filtration section. The filtration section consisted of two stainless steel pipes (1in ID) attached by two flanges. The filter media was placed in between the two pipes and sealed with foam gaskets. The pressure drop across the filter media was recorded using a pressure transducer by Omega. The filtration efficiency was calculated by using the particle count data recorded by Laser Aerosol Spectrometer (LAS-XII) from TSI. LAS-XII spectrometer can detect particles with diameter ranging from 90 to 7500 nm within 99 channels. The sampling flow rate can be set between 10 sccm to 100 sccm, and 50 sccm was used for this

study. The flow meters were adjusted to get a face velocity of 53.2 cm/s for all tests. The concentration of salt in the nebulizer was 5% (w/w).

4.2.3 Salt Aerosol Concentration

It is important to determine the concentration of salt particle generated by Hudson Nebulizer. The salt concentration can be calculated in parts per million by weight (ppmw), and can be calculated with equation 13, where c_{salt} is the concentration of salt in ppmw, m_{salt} is the mass of sea salt (g) and m_{air} is the mass of air (g).

$$c_{salt} = \frac{m_{salt}}{m_{air}} * 10^6 \qquad Equation\ 13$$

Donaldson media was used as a filter media. It was assumed that all particles would be captured when the media was clogged. The difference in the mass of clogged media and clean media would give the mass of salt particulates captured from the upstream. This mass was calculated as $m_{salt} = 8.34 \times 10^{-3}$ g. The total volume of air during mass increase was 324 liters at 53.2 cm/s within 20 mins. Hence the salt concentration in the aerosol upstream was calculated as

$$c_{salt} \approx \frac{8.34*10^{-3}}{(324/22.4)*29} (* 10^6) = 19.8 \text{ ppmw}$$

4.2.4 Filtration Performance Metrics Used

The filtration performance metrics used in this chapter are filtration efficiency and Quality Factor.

4.2.4.1 Filtration Efficiency

The filtration efficiency is the most important metric used to measure the performance of a filter. It primarily depends on type of filter media used. It also depends on particle size of filtrate, filtration area and filtration velocity. The average filtration efficiency can be evaluated

using equation 14, according to ASHRAE 52.2 Standard[17]. It is expressed as a number between 0 and 1.

$$E = \left(\frac{n_{up} - n_{down}}{n_{up}}\right) \qquad Equation\ 14$$

4.2.4.2 Quality Factor

Filtration process consumes energy in the form of pressure drop (i.e. PV work). The cost-benefit ratio of filtration process is defined in terms of Quality Factor, which is defined by equation 15. The Quality Factor is fundamentally defined as filtration efficiency divided by the pressure drop through the media. Quality Factor can also be defined as the ratio of fractional capture of particles per unit thickness divided by the pressure drop per unit thickness.

$$QF = \frac{\gamma}{\Delta P/_t} = \frac{\gamma t}{\Delta P} = \frac{\ln(1/P)}{\Delta P} = -\frac{\ln\left(\frac{1}{E}\right)}{\Delta P} \qquad Equation\ 15$$

where γ is the fractional capture of particle per thickness (dimensionless), t is filter thickness in m, ΔP is pressure drop across the filter in Pa, E is the total filtration efficiency (dimensionless).

The Quality Factor can depend on many variables including: gas temperature, gas pressure, gas face velocity, gas viscosity, RH, particulate size, particulate composition, particulate shape and many filter properties including fiber diameter, composition, orientation, volume loading, media thickness, hydrodynamic entrance, exit conditions etc. The Quality Factor incorporates the fundamental filtration mechanisms discussed in previous chapters.

4.3 Results

The results for filtration efficiency and Quality Factor for AU Toyobo 1600 Felt Nano-floc media with different amount of PTFE coatings for experiments conducted at different RH levels are presented and discussed in the following sections.

4.3.1 Filtration Efficiency and Quality Factor of AU Toyobo 1600 Felt Nano-floc Filter Media with Different PTFE Coatings at 30% RH

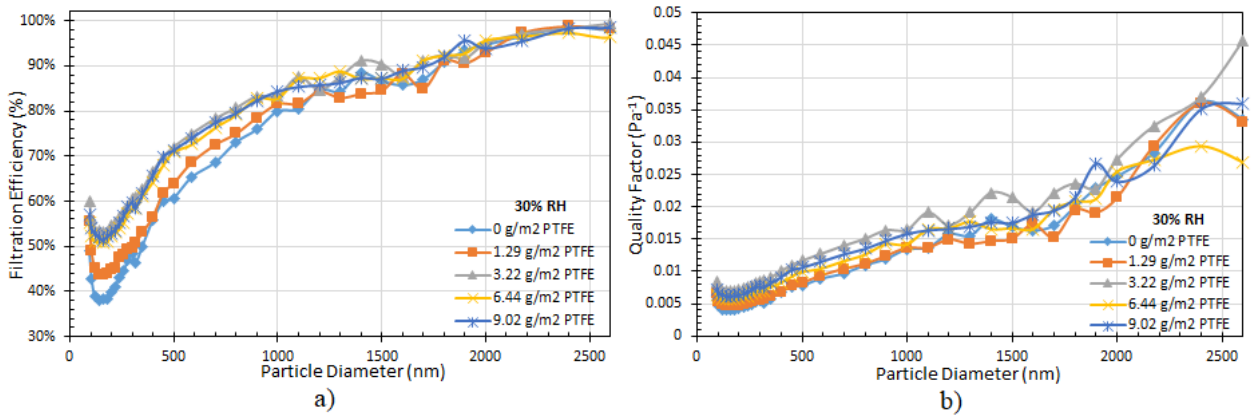

Figure 52. a) Filtration Efficiency b) Quality Factor of AU Toyobo 1600 Felt Nano-floc filter media at 30% RH with different PTFE coatings

30% RH is below the deliquescent point of Sodium Chloride (NaCl). Hence the salt particulates are relatively dry. However, some moisture will be present. For filter media with 0 g/m^2 PTFE coating, some of the low moisture particulates will be captured by the media, but the pores of the activated carbon fibers fill up quickly with moisture leaving less space for salt entrapment. So as seen in Figure 52a, the filtration efficiency curve shows a normal trend, however, the quality factor is the lowest because of the pressure drop caused due to cake filtration by the moist filter. Any subsequent particulates will be entrapped by surface filtration mechanism, not by volume filtration mechanism. As PTFE coating was increased from 0 g/m^2 to 9.02 g/m^2, more water was kept off the filter, improving salt penetration as indicated by improved filtration efficiency curves in Figure 52a. However, as the PTFE coating increases, the pressure drop across the media also increases due to blockage of the surface by PTFE layer. 9.02 g/m^2 PTFE has the highest filtration efficiency, but this enhancement in efficiency comes with high pressure drop penalty. Therefore, 9.02 g/m^2 PTFE coated sample does not have the highest quality factor. The

optimal PTFE coating was 3.22 g/m^2 at 30% RH, since it had the highest quality factor among all samples studied. This means that the pressure drop associated with coating 3.22 g/m^2 is warranted with improvement in filtration efficiency.

4.3.2 Filtration Efficiency and Quality Factor of AU Toyobo 1600 Felt Nano-floc Filter Media with Different PTFE Coatings at 50% RH

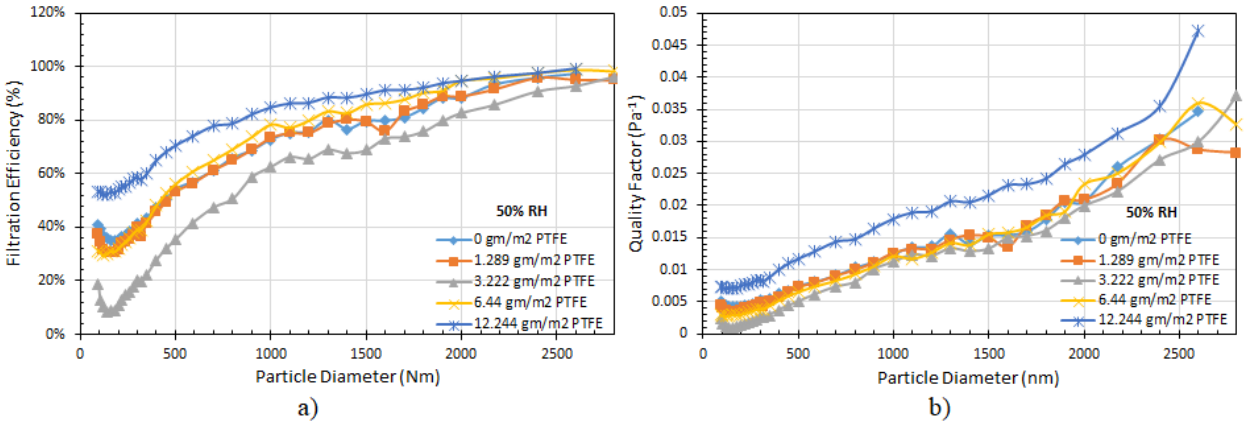

Figure 53. a) Filtration Efficiency b) Quality Factor of AU Toyobo 1600 Felt Nano-floc filter media at 50% RH with different PTFE coatings

50% RH is still below the deliquescent point for NaCl. However, the moisture content is more than that compared to 30% RH. At 50% RH some particulates are in the form of hydrated salt, while some particulates are in the form of tiny salt droplets. PTFE was coated in the range from 0 g/m^2 to 12.2 g/m^2. Filtration efficiency did not improve with 1.28 g/m^2 PTFE coating, as shown in Figure 53a. The filtration efficiency further decreased with 3.22 g/m^2 PTFE compared to 0 g/m^2 PTFE, and this anomalous decrease could be due to possible PTFE contamination inside the depth of the filter, resulting in bypassing of salt particulates all together. Experiments need to be repeated for 3.22 g/m^2 PTFE coated sample to further verify this phenomenon. The 6.44 g/m^2 PTFE sample's filtration performance was also comparable to 0 g/m^2 PTFE. Only for 12.2 g/m^2 PTFE coated sample, the filtration efficiency was better than the 0 g/m^2 PTFE sample. This can

be attributed to the hydrophobic PTFE keeping the water off the media, improving salt penetration into the depth consequently increasing filtration efficiency.

Regarding quality factor, the 0 g/m^2 PTFE coated sample showed similar performance as samples with up to 6.44 g/m^2 PTFE coating, as shown in Figure 53b. It is because the filtration efficiency did not improve for these samples, the pressure drop also did not increase. However, the 12.2 g/m^2 PTFE showed much higher quality factor compared to the rest of the samples. It is most likely due to the 12.2 g/m^2 PTFE sample having enough hydrophobicity to prevent all water from sea salt aerosol to flood the media, resulting in improved penetration of salt particulates into the depth of the media without high pressure drop. There should be an upper limit on the amount of PTFE coating because after certain amount of coating, the pressure drop will start increasing significantly due to formation of PTFE layer on the media, increasing the resistance for the flow.

4.3.3 Filtration Efficiency and Quality Factor of AU Toyobo 1600 Felt Nano-floc Filter Media with Different PTFE Coatings at 72% RH

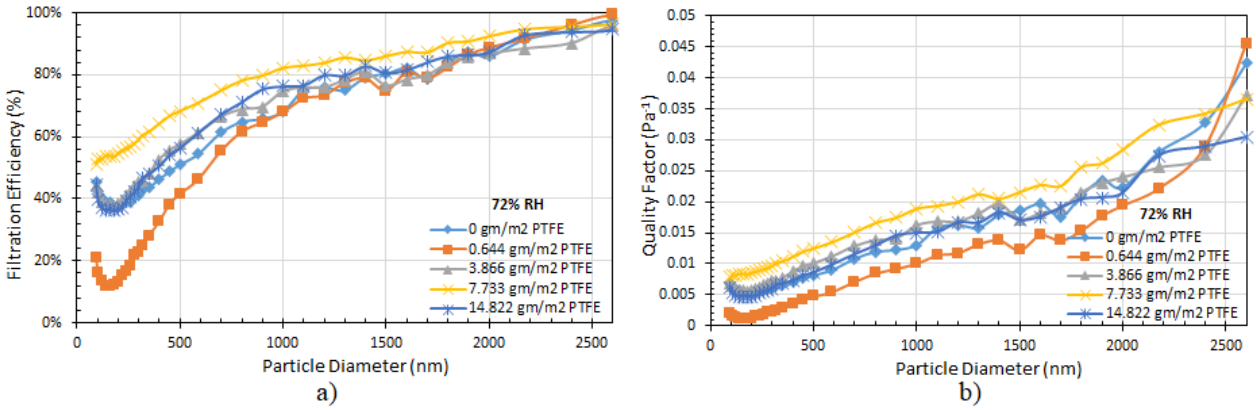

Figure 54. a) Filtration Efficiency b) Quality Factor of AU Toyobo 1600 Felt Nano-floc filter media at 72% RH with different PTFE coatings

72% is the deliquescent point for NaCl particulates. At this RH, the NaCl particulates absorbs water and acts as tiny droplets. Although the salt content is the same, the particle size

increases due to swelling. The filtration efficiency curves, as shown in Figure 54a, shows that an optimal coating of PTFE i.e. 7.73 g/m^2 has the highest filtration efficiency. The filtration efficiency of 0.64 g/m2 PTFE is the lowest for 0 to 900 nm diameter range. The filtration efficiency showed marginal improvement for 3.86 g/m^2 PTFE. However, any increase in PTFE coating beyond the optimal value of 7.73 g/m^2, did not show any improvement in filtration efficiency. The 14.82 g/m^2 PTFE sample had filtration efficiency values similar to that of 0 g/m^2 PTFE sample.

The quality factor at 72% RH for all samples are shown in Figure 54b. The sample with 7.73 g/m^2 PTFE, which also demonstrated the highest filtration efficiency, also has the highest quality factor. This can be attributed to the optimal PTFE coating, keeping water off the media and allowing better penetration of salt particulates into the depth of media, without increasing pressure drop significantly. The quality factor values for 0 g/m^2, 3.86 g/m^2, and 14.82 g/m^2 were similar across the entire particle diameter range. Since salt particulates are heavily moisturized in the ocean environment, the optimal PTFE coating of 7.73 g/m^2 will greatly enhance the filtration media performance and help increase the lifetime of the filter.

4.4 Conclusion

Salt aerosol behave differently in different RH environment. Work from previous chapter showed that some amount of PTFE coating improved the particle loading capacity. However, the filtration efficiency and Quality Factor were not studied in detail. In this chapter, filtration experiments were performed at low, medium and high RH environment for samples with different amounts of PTFE coatings. At low RH value, i.e. 30%, 3.22 g/m^2 of PTFE coating yielded the highest Quality Factor for AU Toyobo 1600 Felt Nano-floc filter. At medium RH value, i.e. 50%, AU Toyobo 1600 Felt Nano-floc filter with 12.2 g/m2 PTFE yielded the highest Quality Factor. The most relevant RH level is 72% since it is similar to that of the ocean environment. At

72% RH, AU Toyobo 1600 Felt Nano-floc filter with 7.73 g/m2 PTFE yielded the highest Quality Factor. These quality factor values have to be used along with the particle loading values from Chapter 3, to design or choose a suitable filter media. Applications requiring high air quality want high particle loading capacity and the pressure drop is not considered that important. However, there are also applications that can compromise with the air quality to some extent, to minimize the energy cost associated with pressure drop. Hence, a judicious decision based on the requirement of air quality can be made using Quality Factor and particle loading curves.

Chapter 5: Future Work

5.1 Pleating and Packaging of AU Nano-floc Filter Media

Filters can be pleated and packaged inside a cassette. Typically, commercial filter media such as Donaldson are pleated as shown in Figure 55. Pleating can improve pressure drop performance and overall capacity of filtration units. Pleating a flat filter media into corrugated arrangement increases the available filtration area which helps decrease the face velocity and consequently pressure drop across the filter. However, the industrial sample is much thinner and has high pleatability compared to AU Nano-floc filter media. Efforts will be performed to study the ease with which the AU Nano-floc filter media can be scaled up, pleated and packaged into filter elements.

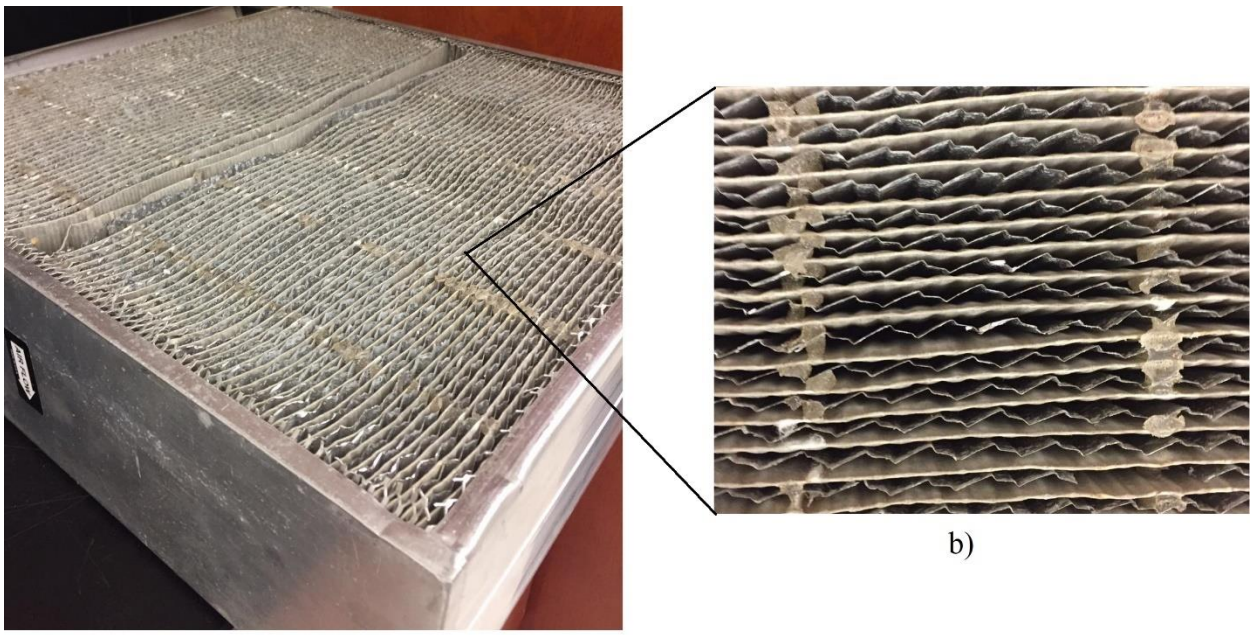

a) b)

Figure 55. a) An opened filter cassette from Donaldson Inc. b) Pleating arrangement of filter media inside the Donaldson filter cassette

Design parameters used in pleating a filter are pleat height, pleat count, media thickness, permeability and filter housing. Finding minimum pressure drop with maximum

filtration area with respect to permeability vs thickness needs to be considered during pleating in order to improve the lifetime of filter and minimize energy cost.

5.1.1 Pressure Drop in a Pleated Media

A theoretical model for pressure drop across a pleated filter has been developed by Sothen.[12] This model was developed by summing individual resistance across pleated filter using Forchheimer-extended Darcy's law and Bernouli's equation, as given by equation 16.

$$\Delta P_F = \frac{1}{2}\rho[(2K_G)V_1^2 + (K_C + K_E + K_P)V_3^2] + AV_4 + BV_4^2 \qquad Equation\ 16$$

where K_G is Grating coefficient of friction, K_P is Pleat coefficient of friction, K_C is coefficient of contraction, K_E is coefficient of expansion. This equation will be used to calculate pressure drop across pleated media for various nano-floc embedded filters mentioned in this thesis.

5.1.2 U-Curve Determination

The resistance versus pleat count graph indicates a lowest obtainable resistance (LOR). The LOR occurs due to tradeoff of media resistance for viscous resistance, as the pleat count is increased, as shown in Figure 56. A similar U-curve will be plotted for different nano-floc filter media that has been introduced in this thesis, to find the optimal pleat count with lowest resistance.

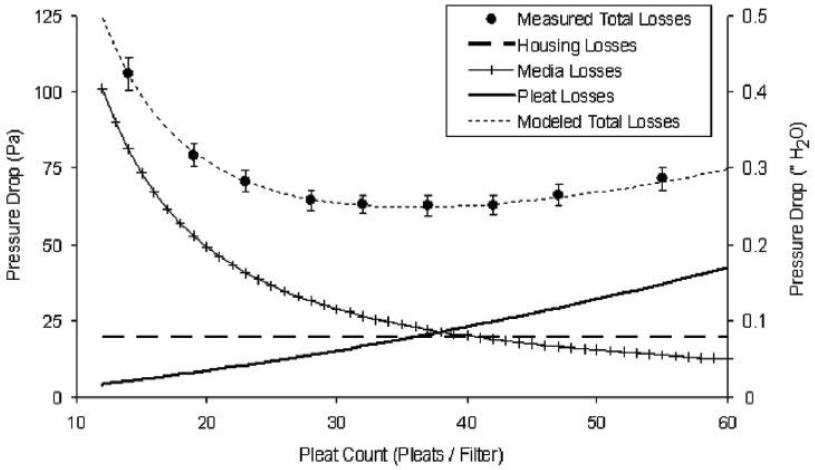

Figure 56. Pressure drop across a pleated filter vs pleat count to find the optimal pleat count

5.1.3 Construction of Multi-Element Structured Array (MESA)

The pleated filter media that is discussed in the previous section can be arranged into a multi element pleated filter banks, as shown in Figure 57. In ocean environment which is high in sea salt loading, single filter elements will clog in unacceptably short period of time. MESA will lessen the filter entrance face velocity and particle loading per filter surface area accordingly. The pressure drop will be reduced due to altered thickness/permeability of the filter. Hence MESA will be constructed for different AU Nano-floc filter media mentioned in this thesis.

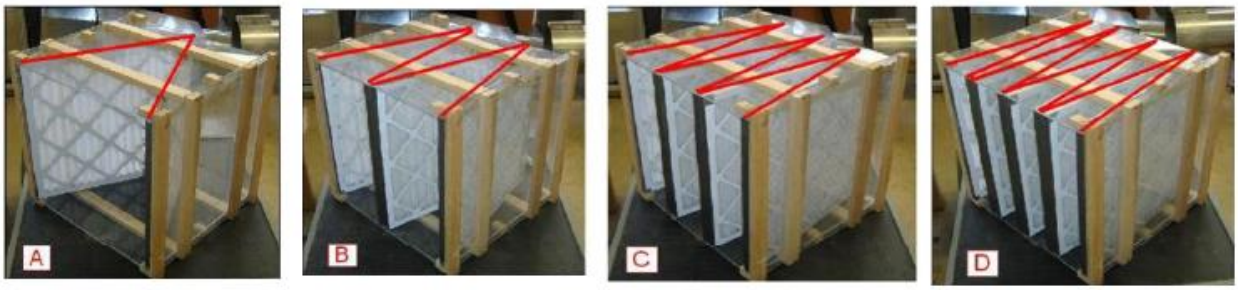

Figure 57. MESA with a) 2 filter (V-shaped) b) 4 filter (W shaped), c) 6 filters (WV shaped) and d) 8 filters (WW shaped) per unit of duct cross-section

A model for pressure drop across MESA was developed by Sothen and is expressed as Equation 17. It was also developed using Bernoulli's equation and Forchheimer-extended Darcy's law.

$$\Delta P_F = \frac{1}{2}\rho[(K_{CB} + K_{EB})V_2^2 + (2K_G + K_S)V_3^2 + (K_{CP} + K_{EP} + K_P)V_5^2] + AV_6 + BV_6^2 \qquad Equation\ 17$$

where K_{CB} is the entrance coefficient of friction, K_{EB} is the exit coefficient of friction and K_S is slot coefficient of friction. A U-Curve will be plotted as shown in Figure 58 to determine

the optimal pleat count with lowest pressure drop for different nano-floc filter media prepared in our lab.

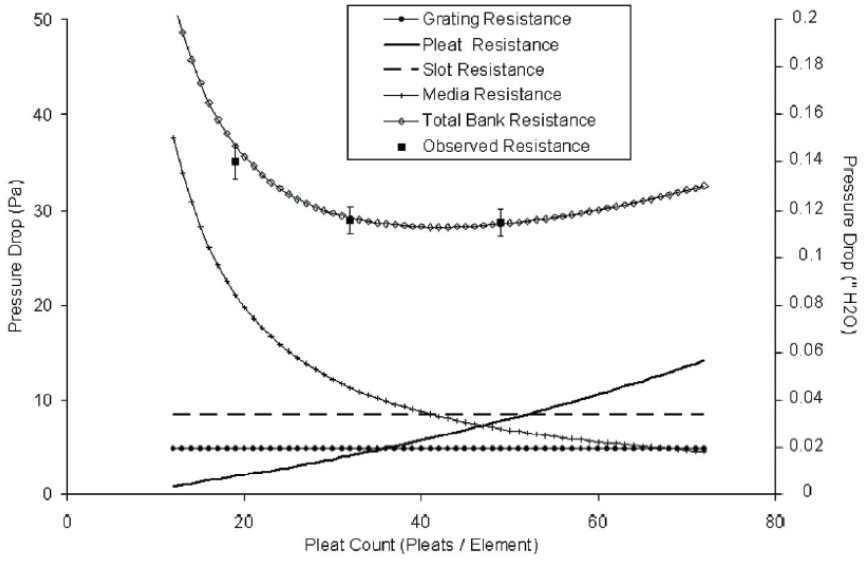

Figure 58. MESA Pleating Curve

Similarly, a plot like Figure 59 with pressure drop vs filtration area for different MESA configuration will be plotted for various nano-floc media mentioned in this thesis.

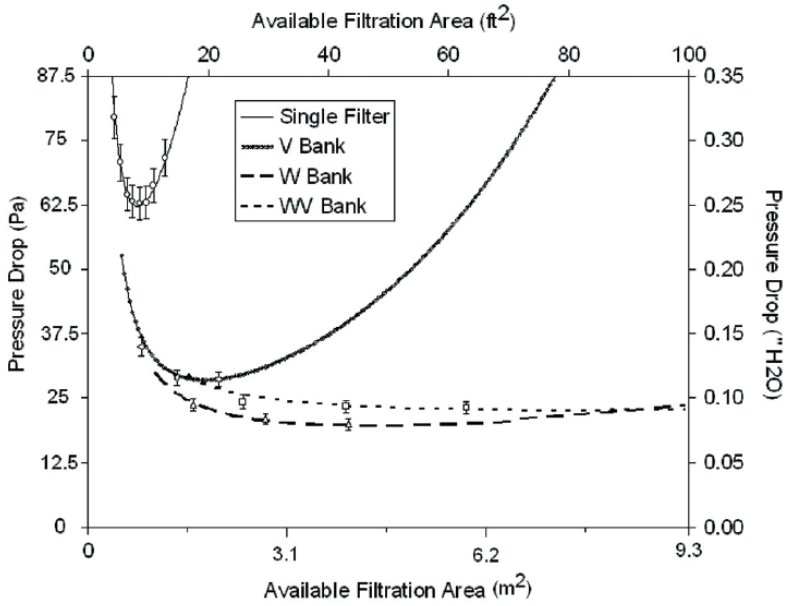

Figure 59. Available area of filter for different MESA configuration

5.2 Understanding the Underlying Forces and Dynamics for NaCl Movement in AU Filter Media

More work will be performed to understand the movement of NaCl particulates into the pores of AU Nano-floc filter media. The RH above the activated carbon will be cycled to study its effect on salt movement into the activated carbon fiber pores. Similarly effect of drying cycles will also be studied. So far regeneration has only been done once, hence more regeneration cycle will be performed to study its effect on salt particulate holding capacity, pressure drop and quality factor.

5.3 Ultra-low PTFE Dilution

Ultra-low concentration of PTFE will be applied to entire filter, including the depth, as opposed to just surface. The filtration experiments will be performed under test conditions relevant to ocean environment. Filtration parameters such as filtration efficiency, quality factor and dirt holding capacity will be studied. Also, an optimal temperature to anneal the PTFE will be determined so that the PTFE does not get washed out during backflush for filter regeneration.

5.4 Durability of AU Nano-floc Filter Media Under Back-Flush Conditions

Back-flushing will be performed on dirt and aerosol loaded filter media to regenerate it. The back-flushing will be examined in both wet and dry conditions, and the effect of hydrophobic and hydrophilic additives will be further assessed.

The durability of the filter media is crucial for regeneration of filter. Experiments will be conducted to study if back-flushing will cause any structural damage to nano-floc filter media developed in our lab. The shedding of the fibers during back-flush operation will also be studied since it is an important safety and performance issue. The nano-floc filter will be exposed to accelerated air flow and the outlet stream will be passed over a separate filter which will be

analyzed for fiber sheds using SEM or EDAX analysis. Furthermore, LAS-XII spectrometer in our lab will also be utilized to study the aerosol content before and after the filter media to see if there is an increase in particles after filter media.

5.5 Journal Articles

Finally, at least two journal articles, one for work pertaining to nano-fiber inclusion, while another for the potential of activated carbon fiber pore volume for salt entrapment will be written and be submitted to reputed scientific journals.

References:

1. Zhao, Pengfei. Experimental Study of Sea Salt Particles (SSP) Filtration Performance for On-Board SOFCs. Auburn University, 7 May 2016.
2. Wilcox, Melissa, et al. Guideline for Gas Turbine Inlet Air Filtration Systems. GMRC, SWRI, Apr. 2010.
3. Brown, R. C. Air Filtration: an Integrated Approach to the Theory and Applications of Fibrous Filters. Pergamon Press, 1993.
4. Spurny, Kvetoslav Rudolf. Advances in Aerosol Filtration. Lewis, 1998.
5. Hinds, William C. Aerosol Technology: Properties, Behavior, and Measurement of Airborne Particles. Wiley, 1999.
6. Davies, C. N. Air Filtration. Academic Press, 1975.
7. Karwa, Amogh N. Aerosol Filtration Enhancement Using Carbon Nanostructures Synthesized within a Sintered Nickel Microfibrous Matrix. Separation and Purification Technology/Elsevier, 25 Nov. 2011.
8. Cahela, Donald R. “Permeability of Sintered Microfibrous Composites for Heterogeneous Catalysis and Other Chemical Processing Opportunities.” ScienceDirect, Elsevier, 21 Sept. 2001.
9. Karwa, Amogh N. “A Novel Nano-Nonwoven Fabric with Three-Dimensionally Dispersed Nanofibers: Entrapment of Carbon Nanofibers within Nonwovens Using the Wet-Lay Process.” IOPScience, Nanotechnology, 13 Apr. 2012.
10. Karwa, Amogh N. “Pressure Drop and Aerosol Filtration Efficiency of Microfibrous Entrapped Catalyst and Sorbent Media: Semi-Empirical Models.” Separation and Purification Technology, Elsevier, 20 Oct. 2011.

11. Fisk, W. J., et al. “Performance and Costs of Particle Air Filtration Technologies.” Wiley Online Library, John Wiley & Sons, Ltd (10.1111), 13 Dec. 2002.
12. Sothen, Ryan A. “A Semi-Empirical Pressure Drop Model: Part I-Pleated Filters.” Taylor & Francis, HVAC&R Research, 25 Feb. 2011.
13. “The Loading of Fibrous Filters with Submicron Particles.” Journal of Aerosol Science, Pergamon, 1991.
14. Laser Aerosol Spectrometer MODEL 3340 Operation and Service Manual. TSI Inc., Sept. 2015.
15. Bénesse, M. “Collection Efficiency of a Woven Filter Made of Multifiber Yarn: Experimental Characterization during Loading and Clean Filter Modeling Based on a Two-Tier Single Fiber Approach.” Journal of Aerosol Science, Pergamon, 6 Dec. 2005.
16. Steffens, J., and J.R. Coury. “Collection Efficiency of Fiber Filters Operating on the Removal of Nano-Sized Aerosol Particles: II. Heterogeneous Fibers.” Separation and Purification Technology, Elsevier, 10 July 2007.
17. ASHRAE 52.2. Method of Testing General Ventilation Air-Cleaning Devices for Removal Efficiency by Particle Size. ASHRAE, 1992.
18. Faulkner, B D, et al. Life-Cycle Costing of Air Filtration. ASHRAE Journal 47:30-32, 2005.
19. Inagaki, Michio, et al. “Heavy Oil Sorption and Recovery by Using Carbon Fiber Felts.” Carbon, Pergamon, 9 Jan. 2002.
20. Nishi, Yoko, et al. “Evaluation of Sorption Behavior of Heavy Oil into Exfoliated Graphite by Wicking Test.” Journal of the Society of Materials Science, Japan, The Society of Materials Science, Japan, 3 June 2009.

21. Nishi, Yoko, et al. “Sorption Kinetics of Heavy Oil into Porous Carbons.” Water Research, Pergamon, 12 Oct. 2002.
22. Alcaniz-Monge, Juan, and Angel Linares-Solano. Mechanism of Adsorption of Water in Carbon Micropores As Revealed by a Study of Activated Carbon Fibers. The Journal of Physical Chemistry B, 3 May 2002.
23. Iiyama, T., and K. Nishikawa. An Ordered Water Molecular Assembly Structure in a Slit-Shaped Carbon Nanospace. The Journal of Physical Chemistry, 1 June 1995.
24. Iiyama, T., et al. Organized Molecular States in Carbon Micropores. Springer, Boston, MA, 1 Jan. 1996.
25. Iiyama, T., and T. Suzuki. An Imperfect Packing of CCl4 Molecules Confined in a Graphic Slit Nanospace. Chemical Physics Letters, 13 Aug. 1996.
26. Liu, Lumeng, et al. Water Adsorption on Carbon - A Review. Advances in Colloid and Interface Science, 10 Nov. 2017.
27. Xiao, Jing, and Zhenlong Liu. S/O-Functionalities on Modified Carbon Materials Governing Adsorption of Water Vapor. The Journal of Physical Chemistry, 1 Oct. 2013.
28. Horikawa, Toshihide, and Noriyuki Sakao. “Preparation of Nitrogen-Doped Porous Carbon by Ammonia Gas Treatment and the Effects of N-Doping on Water Adsorption.” Carbon, Pergamon, 23 Dec. 2011.
29. Figueiredo, José Luís. “Functionalization of Porous Carbons for Catalytic Applications.” Journal of Materials Chemistry A, The Royal Society of Chemistry, 8 Apr. 2013.

30. Fletcher, A.J., and Y. Uygur. Role of Surface Functional Groups in the Adsorption Kinetics of Water Vapor on Microporous Activated Carbons. The Journal of Physical Chemistry, 23 May 2007.
31. Nakamura, M., et al. Equilibration-Time and Pore-Width Dependent Hysteresis of Water Adsorption Isotherm on Hydrophobic Microporous Carbons. Carbon-Pergamon, 8 Sept. 2009.
32. Horikawaa, Toshihide, et al. Effects of Temperature on Water Adsorption on Controlled Microporous and Mesoporous Carbonaceous Solids. Carbon-Pergamon, 12 Jan. 2013.
33. Ohba, Tomonori, et al. Cluster-Growth-Induced Water Adsorption in Hydrophobic Carbon Nanopores. The Journal of Physical Chemistry B, 25 Aug. 2004.
34. Ohba, Tomonori, et al. Structures and Stability of Water Nanoclusters in Hydrophobic Nanospaces. Nano Letters, 8 Jan. 2005.
35. Karwa, Amogh N. Aerosol Filtration Performance of Novel 3-Dimensional Nonwoven Composites. Auburn University, 30 Dec. 2012.
36. Ebnesajjad, Sina, and Cyrus F. Ebnesajjad. Surface Treatment of Materials for Adhesive Bonding. 2nd ed., William Andrew, 2014.
37. Rahnejat, Homer. Tribology and Dynamics of Engine and Powertrain. Woodhead Publishing, 30 Sept. 2010.
38. Sarp, Sarper, and Nidal Hilal. Membrane-Based Salinity Gradient Processes for Water Treatment and Power Generation. Elsevier, 20 July 2018.
39. Huang, Fenglin, et al. Surface Functionalization of Silk Fabric by PTFE Sputter Coating. Journal of Material Science, 5 Feb. 2007.

40. Alagirusamy, R., and A. Das. Technical Textile Yarns, Industrial and Medical Applications. Woodhead Publishing, 2010.
41. Montgomery, James F., et al. Impact of Relative Humidity on HVAC Filters Loaded with Hygroscopic and Non-Hygroscopic Particles. Taylor & Francis/Aerosol Science and Technology, 22 Feb. 2015.
42. Aerosol Statistics Lognormal Distribuions and DN/DlogDp, Application Note PR-001. TSI Inc., 2012.